

**SIMULATION ON EDDY CURRENT DAMPER AND ITS REGENERATIVE
BEHAVIOUR IN SHOCK ABSORBER FOR ELECTRIC VEHICLE**

YONG YEW RONG

**A project report submitted in partial fulfilment of the
requirements for the award of Bachelor of Engineering
(Hons.) Mechatronics Engineering**

**Faculty of Engineering and Science
Universiti Tunku Abdul Rahman**

APRIL 2013

DECLARATION

I hereby declare that this project report is based on my original work except for citations and quotations which have been duly acknowledged. I also declare that it has not been previously and concurrently submitted for any other degree or award at UTAR or other institutions.

Signature : _____

Name : YONG YEOW RONG

ID No. : 09UEB08741

Date : 6th May 2013

APPROVAL FOR SUBMISSION

I certify that this project report entitled “**SIMULATION ON EDDY CURRENT DAMPER AND ITS REGENERATIVE BEHAVIOUR IN SHOCK ABSORBER FOR ELECTRIC VEHICLE**” was prepared by **YONG YEW RONG** has met the required standard for submission in partial fulfilment of the requirements for the award of Bachelor of Degree (Hons.) Mechatronics at Universiti Tunku Abdul Rahman.

Approved by,

Signature : _____

Supervisor: Assoc. Prof. Dr. Chew Kuew Wai

Date : 7th May 2013

The copyright of this report belongs to the author under the terms of the copyright Act 1987 as qualified by Intellectual Property Policy of University Tunku Abdul Rahman. Due acknowledgement shall always be made of the use of any material contained in, or derived from, this report.

© 2013, Yong Yew Rong. All right reserved.

Specially dedicated to
my beloved family, lecturers and friends

ACKNOWLEDGEMENTS

I would like to thank everyone who had contributed to the successful completion of this project. I would like to express my gratitude to my research supervisor, Assoc Prof. Dr. Chew Kuew Wai for his invaluable advice, guidance and his enormous patience throughout the development of the research.

In addition, I would also like to express my gratitude to my loving parents and friends who had helped and given me encouragement and motivation to carry on the research.

SIMULATION ON EDDY CURRENT DAMPER AND ITS REGENERATIVE BEHAVIOUR IN SHOCK ABSORBER FOR ELECTRIC VEHICLE

ABSTRACT

Electric Vehicle uses battery pack as energy storage that has limited capacity hence besides increasing the energy usage efficiency of the vehicle, harvesting regenerative energy from braking or shock absorbing may help to prolong the driving range of the EV. This paper briefly describes the reason for the uprising of Electric Vehicle and some of the existing energy regenerative suspension system while proposed a new hybrid damper. Currently, there are many new designs of the shock absorber that uses other method other than fluid friction. Instead of coming out with a new method, it is possible to combine existing technology to form a new hybrid shock absorber. Eddy current damper has the advantage of contactless damping that does not required physical contact to produce a damping force in which can prolong the life of the damper itself. It will not have problem with fluid leakage nor affected by the rise in temperature. The magnetic flux between the magnet and the conductor inside an eddy current damper can be used to generate power. Ball Screw suspension has higher regenerative efficiency compared to others and good damping control. By merging these two technologies, it is possible to compensate each of their disadvantages and take hold on their advantages. In current project, the history of electric vehicle is briefly introduced. After that, a quick study on damping ratio is done to understand the working principle of a shock absorber. Lastly, the concept, design and idea of the new hybrid damper are briefly introduced and simulation is mainly done on the eddy current damper component to show the possibility of the new design.

TABLE OF CONTENTS

DECLARATION	ii
APPROVAL FOR SUBMISSION	iii
ACKNOWLEDGEMENTS	vi
ABSTRACT	vii
TABLE OF CONTENTS	viii
LIST OF TABLES	x
LIST OF FIGURES	xi
LIST OF SYMBOLS / ABBREVIATIONS	xiii
LIST OF APPENDICES	xv

CHAPTER

1	INTRODUCTION	1
	1.1 Introduction	1
	1.2 Aims and Objectives	2
	1.3 Problem Statement: Disadvantage of Hydraulic Dampers	3
	1.4 Brief History of Electric Vehicle	3
2	LITERATURE REVIEW	5
	2.1 Regenerative Shock Absorber	5
	2.1.1 Hydraustatic Storage Suspension	5
	2.1.2 Battery Coil Induction Suspension	7
	2.1.3 Rack and Pinion Shock Absorber	8
	2.1.4 Ball Screw Shock Absorber	8
	2.1.5 Linear Motion Shock Absorber	10

2.1.6	Hydraulic Transmission Electromagnetic Energy – Regenerative Shock Absorber	11
2.1.7	Eddy Current Damper	13
2.2	Summary of Literature Review	14
3	METHODOLOGY	15
3.1	Modelling of a Shock Absorber	15
3.1.1	Damping ratio	19
3.2	Hybrid Eddy Current Damper	21
3.2.1	Sizing Topology	23
3.3	Eddy Current Damper	23
3.3.1	Strength of Eddy Current	24
3.3.2	Eddy Current Damping Coefficient	24
3.3.3	Magnet Array Configuration	25
3.3.4	Eddy Current Damping Force	26
3.4	Sizing of magnet	28
3.4.1	Magnet Size	30
3.5	Sizing of Copper & Iron Cylinder	33
3.6	Energy Regeneration	34
4	RESULTS AND DISCUSSIONS	36
4.1	Magnet Size	36
4.2	Sizing of Copper Cylinder	37
4.3	Sizing of Iron Cylinder	40
4.3.1	Energy Regeneration	43
5	CONCLUSION AND RECOMMENDATIONS	45
5.1	Hybrid Shock Absorber	45
5.2	Recommendation	45
	REFERENCES	47
	APPENDICES	49

LIST OF TABLES

TABLE	TITLE	PAGE
3.1	General solution of $x(t)$ with different damping ratio	19
3.2	Dimension range of a typical shock absorber	23
3.3	Comparison of different Permanent Magnet Configuration	26
3.4	Magnetic Characteristic of N52 and N54 Grade magnet(2010 – 2015 THMAG Tianhe Advanced)	33
4.1	Different sets of value for $P_C > \approx 1.0$	36
4.2	Reluctance of the magnetic circuit with different iron thickness	42
5.1	Summary of the Eddy Current Damper for hybrid damper	45

LIST OF FIGURES

FIGURE	TITLE	PAGE
2.1	Hydraustatic Storage suspension	6
2.2	Battery Coil Induction Suspension	7
2.3	Rack and Pinion Shock Absorber	8
2.4	Ball Screw Shock Absorber	10
2.5	Linear Motion Shock Absorber by Bose	11
2.6	Hydraulic Transmission Electromagnetic Energy-Regenerative Shock Absorber	12
2.7	Inside of a GenShock shock absorber	13
2.8	Passive EMS proposed by Ebrahimi	14
3.1	Conventional Shock Absorber	16
3.2	Simplified Model of a quarter car (SDOF)	16
3.3	System Sketch and Free Body Diagram of quarter car model	16
3.4	Types of damping and its waveform.	20
3.5	Hybrid Damper	21
3.6	Free Body Diagram of a Hybrid Damper	22
3.7	Different Permanent Magnet Configuration. a) Axially, b) axially and radially, c) radially (inward and outward), and d) radially(outward) magnetized Permanent Magnets	26
3.8	Half lumped model of Eddy Current Damper	29

3.9	Equivalent circuit for one pole pair of the lumped model.	29
3.10	Quick Comparison Chart of 4 types of magnets (2000 Magnet Sales & Manufacturing Company. Inc.)	31
3.11	Demagnetization Curves at Different Temperature for N52 grade magnet. (2010 – 2015 THMAG Tianhe Advanced)	32
3.12	Demagnetization Curves at Different Temperature for N54 grade magnet. (2010 – 2015 THMAG Tianhe Advanced)	32
3.13	Coil placement in the eddy current damper.	35
4.1	Relation between Eddy Current Penetration and Oscillating Frequency	38
4.2	Relation between Current Density and Oscillating Frequency	38
4.3	2d View of Eddy Current simulation to determine the copper width (linear motion)	39
4.4	Relation between Lorentz Force and Copper Thickness with air gap of 5mm with magnet at 7.5T (linear motion)	40
4.5	2d View of Eddy Current simulation to determine the iron width (linear)	41
4.6	Relation between Lorentz Force and Iron Thickness (with air gap of 5mm, Copper thickness of 5mm with magnet at 7.5T)	41
4.7	Velocity profile of damper with copper width, $l_{cu} = 5\text{mm}$ and variable iron width, l_{fe} (mm)	42
4.8	Combination of graph for Oscillation Frequency = 1 Hz, initial velocity = 1m/s	43
4.9	Combination of graph for Oscillation Frequency = 20 Hz, initial velocity = 3m/s	44

LIST OF SYMBOLS / ABBREVIATIONS

a	Acceleration, m/s^2
A_g	Cross-sectional area of the air gap perpendicular to the flux path, m^2
A_m	Cross-sectional Area of the Magnet, m^2
A_w	Area of Conductor Wire, m^2
B	Magnetic Field Strength, W/m^2
B_r	Radial Magnetic Flux Density
c	Damping Coefficient, Ns/m
d	Depth from surface, mm
δ	Depth of Penetration, mm
E	Electric field, N/C
E_i	Induced Voltage, Volts
F	Force, N
F_B	Lorentz Force, N
F_T	Thrust Force, N
f	Frequency of Oscillation, Hz
I	Induced Current, Amperes
J	Depth Current Density, A/m^2
J_i	Current Density, A/m^2
J_s	Surface Current Density, A/m^2
k	Spring Stiffness, N/m
L	Ball Screw Lead, m
L_g	Length of Air Gap, m
L_m	Length of Magnet, m
l_m	Length of Magnet core, mm
l_g	Length of Air Gap, mm
l_s	Length of Air Core, mm

l_{cu}	Thickness of Copper Conductor, mm
l_{fe}	Thickness of Iron Conductor, mm
m	Mass, Kg
P	Power, Watt
R	Resistance, ohms
T	Thickness of Magnet and Pole, mm
T_m	Thickness of Magnet, mm
T_{mg}	Torque caused by magnet, N/m
T_{motor}	Motor Torque, N/m
T_t	Total Torque, N/m
t	Time, s
μ_i	Absolute Permeability of Iron H/m
μ_0	Relative Permeability of Free Space, H/m
μ_{cu}	Absolute Permeability of Copper, H/m
V	Volume, m ³
v	Velocity, m/s
v_z	Vertical Velocity, m/s
ω_0	Natural Frequency, Hz
x	Displacement, m
\dot{x}	Velocity, m/s
\ddot{x}	Acceleration, m/s ²
σ	Electrical Conductivity, S/m
ζ	Damping Ratio
k	Ratio
P_C	Permeance of Coefficient
η	Efficiency
EV	Electric Vehicle
IC	Internal Combustion
EMS	Electromagnetic Suspension

LIST OF APPENDICES

APPENDIX	TITLE	PAGE
	APPENDIX A: Computer Programme Listing	49

CHAPTER 1

INTRODUCTION

1.1 Introduction

Shock absorbers are the essential part of a vehicle suspension system. It is used to smoothen out oscillation caused from driving on uneven road surfaces thus, providing a good ride for the driver and the passengers. It is also designed to maintain contact between the vehicle's tire and the road to provide good handling. Without shock absorbers, travelling safely and comfortably at speeds that would, even on good roads, is quite impractical.

There are several methods used for shock absorbers in automobiles such as material hysteresis, dry friction, compressed gas, fluid friction, electro rheological or magneto rheological, and combination of fluid friction with compressed air with fluid friction the most widely used approach for vehicle dampers world-wide. Examples of dampers using fluid friction are the mono-tube absorber and the twin-tube absorber which are commonly found in most commercial vehicles. Fluid damper is not the most ideal method but it is good enough for most vehicles considering the cost.

Shock absorbers can also be categories into 3 types which are passive, semi-active and active. Passive shock absorbers are dampers with fixed damping ratio and consist of mechanical components only. Active shock absorbers are dampers that require power to run. It is highly adaptive as it is able to change its damping ratio. It consists of mechanical components, electronics and electrical components. Semi-

active shock absorbers are dampers that could run with or without power. It works as a passive damper without power and active with power thus saving power when active functions are not needed. Active suspension has wide range of damping force and can achieve the best performance but it is costly, heavier and power consuming. Semi-active dampers are less costly and less power consuming than active dampers with reduced performance. Passive dampers are dampers without the use of any controller and do not require any power to function at all. The dampers performance is just enough for a vehicle but due to the cost it is mainly used for commercial vehicle.

The name shock absorbers do not actually mean that the device absorbs shocks but rather converts oscillation energy to another form. All dampers basically resist motion via friction. The damper turns the kinetic energy (upward downward motion of the vehicle) into heat which is dissipated into the environment. Fluid damper such as mono-tube shock absorber consists of a spring and a dashpot. The spring stores the energy from the excitation of the wheel base while the dashpot which is basically an oil filled cylinder dissipates the energy. The stored energy is converted into heat via fluid friction between the oil and the walls of the cylinder. Because of this simple concept, fluid dampers are the most popular method, lowest cost and easily manufactured.

1.2 Aims and Objectives

The main objective of this project is to design a new shock absorber that is able to generate electricity for electric vehicles. This project aims to use alternate method other than fluid friction to see its possibility as a shock absorber with the capability to generate electricity.

1.3 Problem Statement: Disadvantage of Hydraulic Dampers

The fluid dampers found in automobile are also known as hydraulic damper. Light mineral oil is usually selected as the damper fluid. The damper oil contains sulphur compounds, giving it a lingering noxious smell. The main parameters of the damper oil are density and viscosity which are very temperature dependent. In a damper, the viscosity helps with lubrication. Lower viscosity oils would perform well, but have a higher vapour pressure and would be prone to cavitations. The increase in temperature reduces the viscosity of the fluid which reduces the damping force. Besides that, the rise in temperature will give a reduction in the density of the fluid which in turn would reduce the damping force. Addition to that, a small leakage on the damper will greatly reduce the performance of the shock absorber.

The main problem with the typical fluid damper is overheating. Overheating of the fluid dampers causes the oil in the dashpot to vaporise thus reducing the viscosity of the fluid which severely decreases the damping effect of the dashpot. The problem of vaporising of damping fluid is solved by introducing pressurized inert gas into the oil chamber restricts the damping fluid from vaporizing at lower temperature thus improving the reliability of the damper. However, there are still possibilities of damper leakage which renders the damper useless.

1.4 Brief History of Electric Vehicle

The first electric vehicles of the 1830s used non-rechargeable batteries. By the end of the 19th century, electric vehicles became widely used with the mass production of rechargeable batteries. At the start of the 20th century, electric vehicle was relatively reliable and started instantly as internal combustion engine vehicles were at that time unreliable, smelly and needs manual cranking to start. The steam engine vehicle which is the other main contender needed lighting and the thermal efficiency of the engines was relatively low.

However, by the year 1920s, once cheap oil was widely available and self starter for the internal combustion engine (invented in 1911) had arrived, the IC engine is found to be a better option for powering vehicles. Ironically, the main market for rechargeable batteries was used to start IC engines. The reason that IC engine vehicles were more successful is due to the specific energy of petroleum fuel to that of batteries. (The specific energy of fuels is around 9000Whkg^{-1} while lead acid battery is around 30Whkg^{-1}) Another problem is the time it takes to recharge the batteries. Even with adequate supply of electrical power, it will take several hours to re-charge the lead acid battery whereas 45 litres of petrol can be put into a vehicle in approximately few minutes.

Despite the problems mentioned above, electric vehicles were still been used in the 19th century and early 20th century. Some public transportation such as trolley bus and trains uses electric supply from rails to run. One of the advantages of electric vehicle over combustion engines is mainly that they produce no exhaust emissions and relatively quiet. They also have better efficiencies during start-stop driving while an internal combustion engine becomes very inefficient and polluting. During the latter part of the 20th century, there have been changes made which make the electric vehicle a more attractive option such as; 1. There are increasing concerns about the environment, both in terms of overall emission of carbon dioxide and also the local emission of exhaust fumes which help make crowded towns and cities unpleasant place to live in. 2. There have been improvements in batteries, motors, controllers and vehicle designs.

Ideas & development from the 19th and 20th centuries are no utilised to produce a new range of electric vehicles that are starting to make an impact. Currently, there are six basic types of electric vehicle. 1. The electric vehicle that runs on traditional battery. 2. The hybrid electric vehicle such as Toyato Prius which combines battery and IC engine. 3. Vehicles which use replaceable fuel as the source of energy using either fuel cells or metal air batteries. 4. Vehicles powered by power lines. 5. Vehicle that uses energy directly from solar radiation. 6. Vehicles that sore energy by alternative means such as flywheels or super capacitors which are nearly always hybrids using some other sources of power as well.

CHAPTER 2

LITERATURE REVIEW

2.1 Regenerative Shock Absorber

Regenerative shock absorber is basically a device that is able to recycle energy from “shocks” for other uses while provide the function like any ordinary shock absorber. According to Lin and Xuexun (2010), there are five main types of energy regenerative suspension design which are;

1. Hydraustatic storage suspension
2. Battery coil induction suspension
3. Rack and pinion suspension
4. Ball screw suspension
5. Linear motion suspension.

The types of shock absorber can be categorized into passive, semi-passive and active shock absorber. The author will only focus on reviewing passive and semi-passive type shock absorbers.

2.1.1 Hydraustatic Storage Suspension

Figure 2.1 shows a schematic diagram of hydraustatic storage suspension by Lin and Xuexun (2010). The design of a hydraustatic storage suspension is similar to a conventional hydraulic suspension but with an added hydraulic pump system. The movement of the piston due to external force creates hydraulic pressure which is stored in the energy accumulator. The energy accumulator supplies the hydraulic

power to power-consuming components, such as hydraulic power steering gear. The disadvantage of this system is the extra weight added onto the vehicle. Although hydraulic system is very stable and matured technology, but high sealing techniques and high precision of manufacturing is required which increases the cost. Furthermore, the energy recycling efficiency is low as energy is constantly dissipated as heat throughout the system via fluid friction. It is also not very practical for automobile to store and use energy in the form of hydraulic pressure.

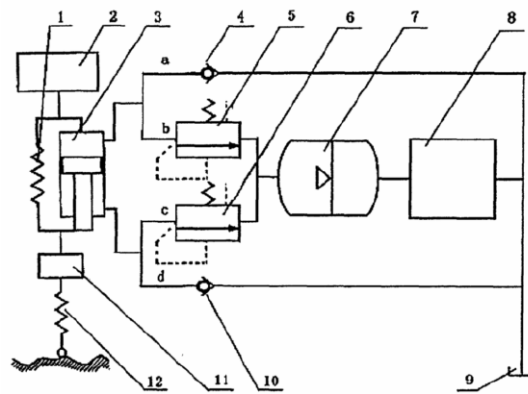


Figure 2.1: Hydraustatic Storage suspension

The main components of hydaustatic storage suspension consists of :

1. spring coil
2. sprung mass
3. piston cavity
4. non-return valve
5. power adaptor
6. power adaptor
7. energy accumulator
8. hydraulic energy-consuming components
9. oil tank
10. non-return valve
11. unsprung-mass
12. stiffness of tyre.

2.1.2 Battery Coil Induction Suspension

Figure 2.2 shows the design for a battery coil induction suspension by He et al. In the design, the typical shock absorber is replaced with a battery coil energy recycling equipment. Shock energy is converted into electrical energy and is stored in batteries. For this suspension, there are a few disadvantages: firstly, because of the pole pitch, to meet a larger damping resistant the suspension system will also need to be larger. Secondly, if the pavement resistance is too great, the magnetic poles might bump into each other, damaging the suspension. Thirdly, the air gap between the magnetic poles is large which may cause a bigger number of coil windings, thus greatly reduces the energy-recycling efficiency.

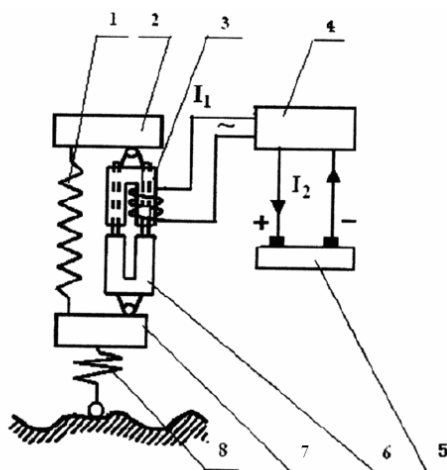


Figure 2.2: Battery Coil Induction Suspension

The main components of battery coil induction suspension consist of:

1. spring coil
2. sprung mass
3. coil
4. rectifier
5. storage battery
6. permanent magnet
7. unsprung-mass
8. stiffness of tyre

2.1.3 Rack and Pinion Shock Absorber

Figure 2.3 shows a rack and pinion shock absorber by chen et al. The conventional shock absorber is replaced by electric motor, a rack and pinion gear. The electric motor is fixed onto the sprung mass and the rack is connected to the unsprung mass. The linear motion between the sprung mass and the unsprung mass will turn the pinion in which turns the motor and generates electricity. The damping force is mainly provided by the back emf of a rotating motor. The pitch size of the rack and pinion will also affect the damping force. The good thing about this design is its high energy regenerative efficiency. However, there is a risk that the rack and pinion might crack and even break if the force on it is too large. On top of that, the constant motion of the rack and pinion generates heat and wears the gear tooth which reduces the performance life of the shock absorber.

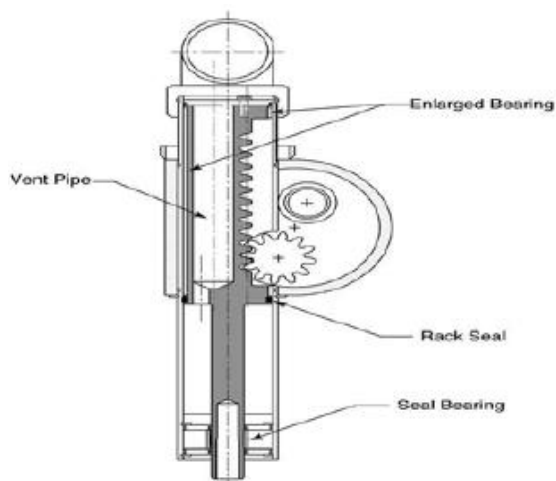


Figure 2.3: Rack and Pinion Shock Absorber

2.1.4 Ball Screw Shock Absorber

Figure 2.4 shows ball screw shock absorber by Zhang et al. The traditional shock absorber is replaced with ball screw gear and it does not require any hydraulic fluid. The ball screw translates the linear motion between the sprung mass and unsprung mass into rotational motion which drives the electric motor and generates electricity.

The idea is similar to rack and pinion suspension in which the damping is provided by electrical motor. Compared with rack and pinion suspension, the ball screw suspension is better in terms of reliability, performance life, size and stability. The only trade off is the damping force of the shock absorber depends on the motor. Generally, larger motor can provide larger damping force but comprises the size. As mentioned by Lin and Xuexun (2010), ball screw energy – regenerative suspension ranks the best among the other suspension mentioned above. However, there are still some defects. Firstly, the damping coefficient is related to the square of transmission ratio, leading to an increase of a given damping coefficient. Similarly, the recycled energy able to absorber by the rotating motor is directly related to the transmission ratio. Secondly, the solid-state joined way of the transmission for the ball screw suspension causes the electric motor to change the rotating direction constantly in accordance to the shock of the system. The rotate speed of the electric motor repeats the cycle of 0 – accelerate – decelerate – 0, which leads to inertia lost. This not only shortens the life of the electric motor, but also gives the electric motor little time to generate electricity during a shock which leads to low energy cycling efficiency. Finally, due to the pure mechanical link structure, the frequency response function of the system to high frequency signals is not zero. This means that the electrical motor will always rotate at any excitation frequency which reduces the damping performance and also the energy recycling performance. However, Zhang et al.(2007), states that the ball screw suspension can achieve good performance of shock isolation from road excitation in low frequencies but the performance was worse than that of passive suspension at high frequencies due to lack of damping force. Liu et al (2011) has proposed a new structure for the ball screw suspension that has no back driving constrain and efficiency of 90% for both driving forward and back driving. According to Montazeri-Gh and Kaviani-pour (2012), ball screw shock absorber is attracting much interest nowadays due to the fact several advantages such as high responsiveness, energy saving performance, controllability and so on.

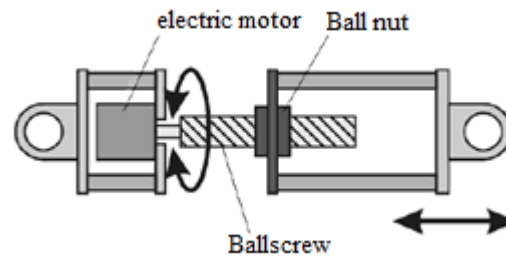


Figure 2.4: Ball Screw Shock Absorber

2.1.5 Linear Motion Shock Absorber

Figure 2.5 show a linear motion shock absorber invented by Bose. In this design, the traditional shock absorber is replaced by a linear electric motor. The advantage of this system is that it requires no intermediary shifting equipments; the kinetic energy is directly converted into electric energy via the linear electric motor. As the vehicle oscillates, a relative displacement takes place between the permanent magnet and the stator coil. From this, the stator coil cuts the magnetic line which generates electricity. The damping force is produced by the counter electromotive force generated by the linear electric motor. This is a type of active Shock absorber which requires power to function. According to Lin and Xuexun (2010), the damping resistance of a linear motor is smaller compared to electric rotating motor due to a larger leakage magnetic flux hence, the linear motion suspension has a plain energy regenerative efficiency. Furthermore, the supporting system for this suspension is more complex and the whole suspension itself is expensive. Currently, only Bose Company applies the linear electric motor as vehicle suspension system.

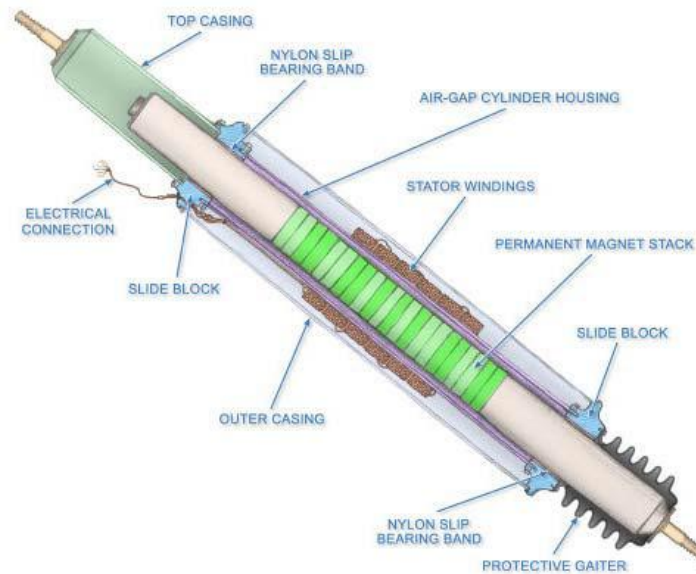


Figure 2.5: Linear Motion Shock Absorber by Bose

2.1.6 Hydraulic Transmission Electromagnetic Energy – Regenerative Shock Absorber

In Lin and Xuexun (2010), the authors proposed a new type of energy-regenerative suspension called “hydraulic transmission electromagnetic energy – regenerative active suspension” as shown in figure 2.6. When a shock causes the hydraulic piston to move up and down, the hydraulic non-return bridge commutates the hydraulic flux brought about by the piston motion into hydraulic flux with unchanging direction vector. This hydraulic flux will go through the energy storage filtration then proceed to drive a hydraulic motor. The damping force of the system is provided by the counter electromotive force produced by the electric motor.

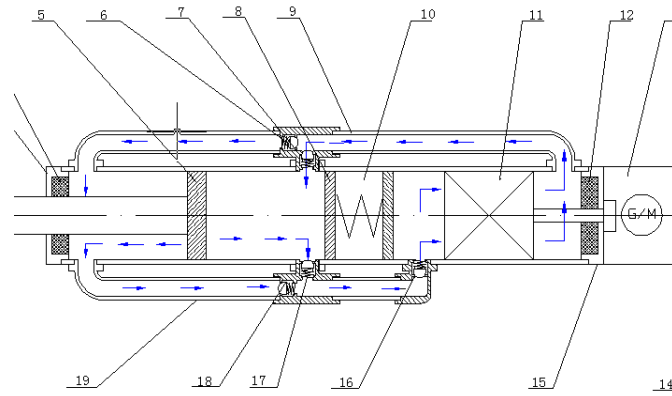


Figure 2.6:Hydraulic Transmission Electromagnetic Energy-Regenerative Shock Absorber

The main parts consist of:

5. piston
6. non-return valve 1
7. non-return valve 2
8. clapboard
9. low pressure pipeline
10. energy accumulator
11. hydraulic motor
16. non-return valve 3
17. non-return valve 4
19. high-pressure pipeline

The advantage of this shock absorber can be summarised as following:

1. The system covers all the shock frequencies as the hydraulic flux flows in one direction towards the motor
2. The electric motor is constantly producing energy when the vehicle is driving.
3. Does not produce a sudden boost in the damping resistance, which makes the system more stable.

A product now in the market called GenShock has been invented by MIT students using almost similar concept. In the opinion of this author, the concept used by both Lin and Xuexun (2010) and GenShock is good as hydraulic fluid provides excellent damping force but in the events of leakage the shock absorber will be render useless.

A slight dent on the shock absorber could also affect the effectiveness of the shock absorber.



Figure 2.7: Inside of a GenShock shock absorber

2.1.7 Eddy Current Damper

Ebrahimi et al. proposed a passive electromagnetic suspension based on eddy current concept. It is a kind of linear motion shock absorber. The suspension consists of permanent magnets with iron pole that act as a translator and a hollow cylinder conductor as stator. The relative motion between the magnets and conductor generates eddy current inside the conductor. Analytical method is used to calculate damping force, and magnetic flux density inside the suspension. The performance is then compared with other commercialised dampers such as magnetorheological dampers and hydraulic dampers. Based on their finding, the performance of eddy current damper is slightly better in terms of vibration control. However, the said suspension cannot totally isolate the vehicle body from vibration. This is due to the fact that the damping force produced is low, can operate on limited bandwidth and have fixed parameters. Figure 2.8 shows the passive EMS proposed by Ebrahimi (2009).

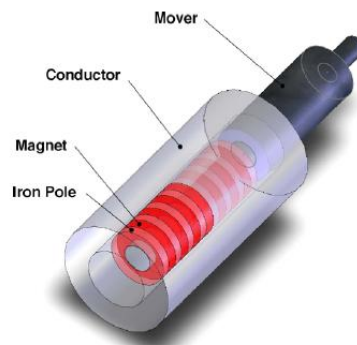


Figure 2.8:Passive EMS proposed by Ebrahimi

2.2 Summary of Literature Review

Based on the review, the author proposed to combine ball screw shock absorber and eddy current damper together to form a new hybrid shock absorber. As mention previously, ball screw shock absorber has high energy regenerative efficiency and has good performance of shock isolation from road excitation at low frequencies. The disadvantage is on its performance was worse than that of passive suspension at high frequencies due to lack of damping force and no energy can be generated at lower speeds. For eddy current damper, it uses contactless damping, and has good vibration control but cannot totally isolate the vehicle body from vibration due to the lack of damping force. By combining the said dampers, it would be possible to increase the damping force.

CHAPTER 3

METHODOLOGY

3.1 Modelling of a Shock Absorber

To illustrate the basic concept of a shock absorber, the author will model the dynamics of a quarter car model to explain the parameters involved in designing a shock absorber. The whole dynamics of a car suspension system is very complex and would take a long time to analysis it, thus, a quarter car model is the start in understanding the dynamics of the system. Moreover, the author's main purpose is to design a different kind of shock absorber and not the whole suspension system. A quarter car modelling will be sufficient to understand the parameter needed to design a shock absorber.

Figure 3.1 shows a conventional shock absorber. It consists of a coil spring and a fluid damper. The function of the coil spring is to absorb impacts while the damper is used to dissipate the energy gained from oscillation. The author will first model the quarter car as a single degree of freedom (SDOF) system to give a general idea on the effect of the parameters on the damping. In this model, the mass of the wheel and the shock absorber is ignored. In figure 3.2, the ' m_{eq} ' represents the equivalent mass or the total mass of a quarter car (includes the passengers). While, ' k_{eq} ' represents the equivalent spring stiffness and ' c_{eq} ' represent the equivalent damping coefficient.



Figure 3.1: Conventional Shock Absorber

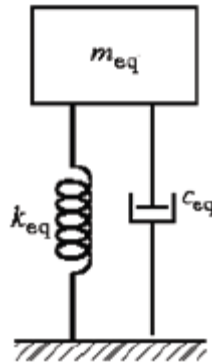


Figure 3.2: Simplified Model of a quarter car (SDOF)

To understand the effects of the parameter of the system, the model will be tested under free vibration. A system is said to undergo free vibration when it oscillates only under an initial disturbance with no external force acting after the initial disturbance. An Ordinary differential equation is formed based on the free body diagram in figure 3.3.

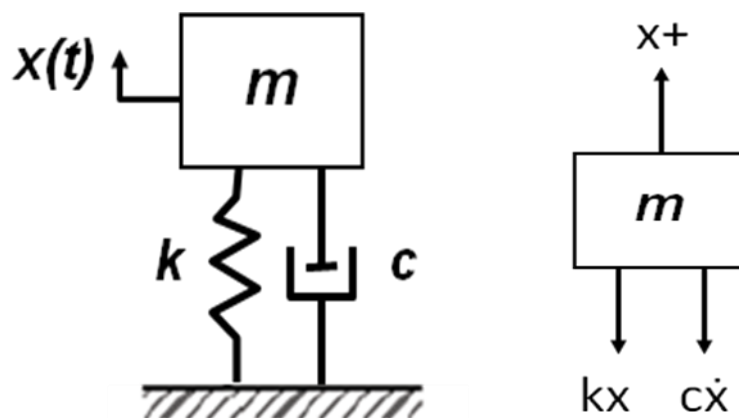


Figure 3.3: System Sketch and Free Body Diagram of quarter car model

From newton's law,

$$\sum F = ma \quad (3.1)$$

$$- c\dot{x} - kx = m\ddot{x} \quad (3.2)$$

$$\ddot{x} + \frac{c}{m}\dot{x} + \frac{k}{m}x = 0 \quad (3.3)$$

where

F = force, N

m = mass, kg

a = acceleration, m/s²

c = damping coefficient, Ns/m

k = spring stiffness, N/m

\ddot{x} = acceleration, m/s²

\dot{x} = velocity, m/s

x = displacement, m

Equation (3.3) can be rewritten as Equation (3.4) :

$$\ddot{x} + 2\zeta\omega_0\dot{x} + \omega_0^2x = 0 \quad (3.4)$$

where

$$\zeta = \frac{c}{2\sqrt{km}}, \text{ damping ratio}$$

$$\omega_0 = \sqrt{\frac{k}{m}}, \text{ natural frequency, Hz}$$

let, $x = Ce^{st}$ and equation (3.4) becomes equation (3.5)

$$s^2 + 2\zeta\omega_0s + \omega_0^2 = 0 \quad (3.5)$$

$$s_{1,2} = \frac{-2\zeta\omega_0 \pm \sqrt{(2\zeta\omega_0)^2 - 4\omega_0^2}}{2} \quad (3.6)$$

Looking for the root for equation (3.5) using equation (3.6) and equation (3.7) is a simplified version of equation (3.6).

$$s_{1,2} = (-\zeta \pm \sqrt{\zeta^2 - 1})\omega_0 \quad (3.7)$$

$$x_1(t) = C_1 e^{s_1 t} \quad (3.8)$$

$$x_2(t) = C_2 e^{s_2 t} \quad (3.9)$$

$$x(t) = C_1 e^{s_1 t} + C_2 e^{s_2 t} \quad (3.10)$$

$$x(t) = C_1 e^{(-\delta + \sqrt{\delta^2 - 1})\omega_0 t} + C_2 e^{(-\delta - \sqrt{\delta^2 - 1})\omega_0 t} \quad (3.11)$$

where

C_1 = undetermined constants

C_2 = undetermined constants

From equation (3.7), the value of damping ratio, ζ will affect the nature of the root s_1 and s_2 in which will affect the behaviour of the solution, equation (3.11). The value of the damping ratio depends on the damping coefficient, c , spring stiffness, k , and mass of the system, m . The damping ratio can never be less than zero as all the constant are positive scalar constants. From equation (3.11), It can also be seen that for $\zeta = 0$ will lead to undamped vibrations.

3.1.1 Damping ratio

A vibration system can be classified based on the damping ratio into three distinct categories which are under-damped ($0 < \zeta < 1$), over-damped ($\zeta > 1$) and critically damped ($\zeta = 1$), each with different effect on the system. Equation (3.5) can be solved or generalized using linear second order differential equation. Table 3.1 summarizes the general solution regarding different damping ratio.

Table 3.1: General solution of $x(t)$ with different damping ratio

Damping Ratio	General Solution, $x(t)$
$0 < \zeta < 1$	$x(t) = e^{-\zeta\omega_0 t} \{C'_1 \cos(\sqrt{1 - \zeta^2} \omega_0 t) + C'_2 \sin \sqrt{1 - \zeta^2} \omega_0 t\}$
	<p>where</p> $C'_1 = x_0$ $C'_2 = \frac{\dot{x}_0 + \zeta\omega_0 x_0}{\sqrt{1 - \zeta^2} \omega_0}$
$\zeta > 1$	$x(t) = C_1 e^{(-\delta + \sqrt{\delta^2 - 1})\omega_0 t} + C_2 e^{(-\delta - \sqrt{\delta^2 - 1})\omega_0 t}$
	<p>where</p> $C_1 = \frac{\omega_0 x_0 (\delta + \sqrt{\delta^2 - 1}) + \dot{x}_0}{2\omega_0 \sqrt{\delta^2 - 1}}$ $C_2 = \frac{-\omega_0 x_0 (\delta - \sqrt{\delta^2 - 1}) - \dot{x}_0}{2\omega_0 \sqrt{\delta^2 - 1}}$
$\zeta = 1$	$x(t) = (C_1 + C_2 t) e^{-\omega_0 t}$
	<p>where</p> $C_1 = x_0$ $C_2 = \dot{x}_0 + \omega_0 x_0$

where

x_0 = value of $x(t)$ when $t = 0$, m

\dot{x}_0 = value of $\dot{x}(t)$ when $t = 0$, m/s

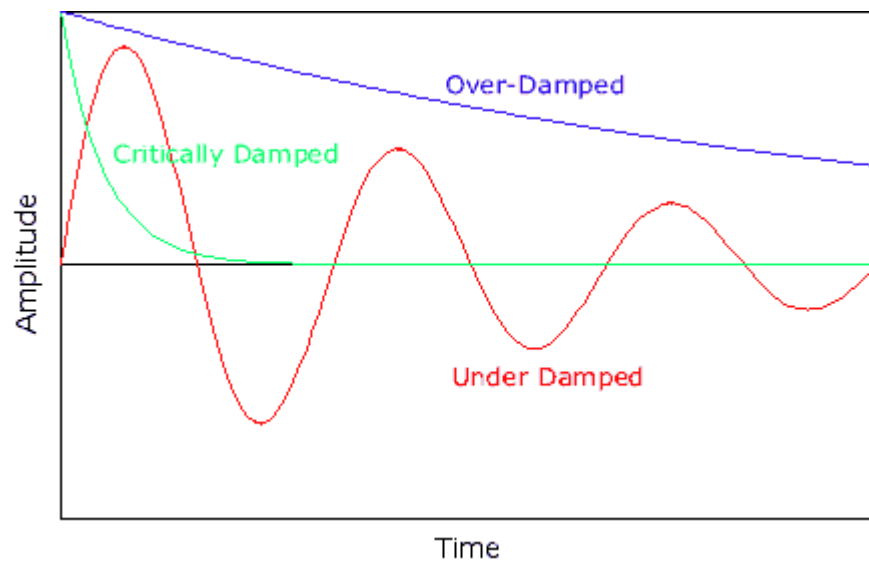


Figure 3.4: Types of damping and its waveform.

Based on figure 3.4, a shock absorber with an over-damped ($\zeta > 1$) characteristic is not desired. It will take a longer time, for the shock absorber to reach its equilibrium than the other two types. Between critically damped ($\zeta = 1$) and under-damped system ($0 < \zeta < 1$), under-damped is more suitable characteristic as an automobile shock absorber as it slowly oscillate back to its equilibrium giving the passengers a gentler cushion.

3.2 Hybrid Eddy Current Damper

Figure 3.5 shows the basic concept of hybrid damper

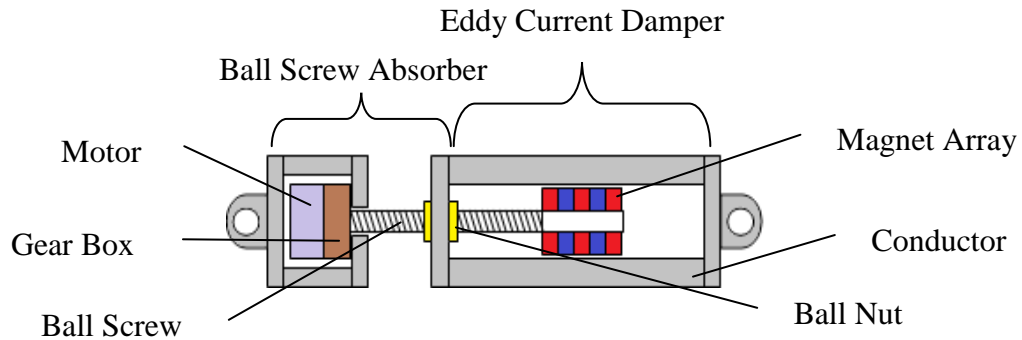


Figure 3.5: Hybrid Damper

In this design, the main purpose of the ball screw absorber component is to generate electricity and to provide extra damping force for the eddy current damper. The authors will be designing an eddy current damper that focuses more on the damping force than the energy regenerative part as that function is mostly taken by the ball screw component.

Figure 3.6 shows the free body diagram of the Hybrid damper. The figure only shows the exerted force, Lorentz force & thrust force. The Lorentz force, F_L is caused by the eddy current effect in the vertical motion while the thrust force is caused by the resisting torque from both the electric motor and eddy current effect in the rotational direction. Forces such as friction forces, gravity forces are not accounted for in the diagram.

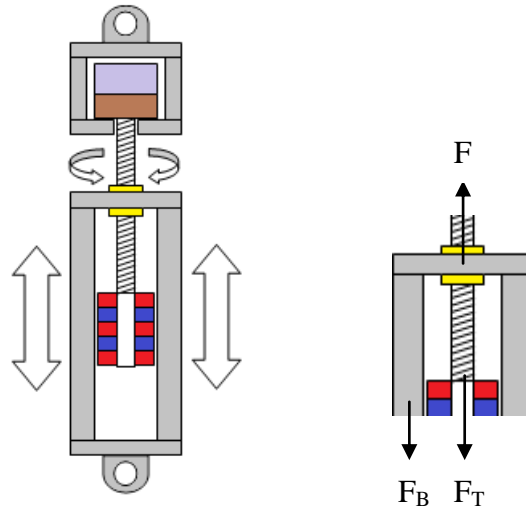


Figure 3.6: Free Body Diagram of a Hybrid Damper

$$F = F_B + F_T \quad (3.12)$$

$$F_B = J_i \times B \quad (3.13)$$

$$F_T = T_t * 2\pi * \eta / L \quad (3.14)$$

$$T_t = T_{motor} + T_{mg} \quad (3.15)$$

where

F = force, N

F_B = Lorentz Force, N

F_T = Thrusting Force, N

η = Efficiency of ballscrew.

L = Lead distant of the ball screw, m

T_t = Total resistive torque, N/m

T_{motor} = Total resistive motor torque, N/m

T_{mg} = Total resistive torque caused by magnet, N/m

3.2.1 Sizing Topology

As the hybrid shock absorber is to be installed in passenger EV, the size should be almost the same as a conventional shock absorber for ease of installation and minimise the trouble with technology compatibility. There is no fixed size for a shock absorber and it depends on the designer. Table 3.2 shows the range of sizes of typical shock absorbers. Table 3.2 shows the dimension range of typical shock absorber. The sizes are just reference with the most important component is the extended length and collapsed length.

Table 3.2: Dimension range of a typical shock absorber

Extended Length, L_1 (cm)	Travel (cm)	Collapsed Length, L_2 (cm)	Diameter 1, d_1 (cm)	Diameter 2, d_2 (cm)
28.83 ~ 64.24	7.11 ~ 24.77	21.72 ~ 39.47	31 ~ 47	30~46

The diagram illustrates a cylindrical shock absorber. It features two circular end caps of different diameters, labeled d_1 on the left and d_2 on the right. The overall length of the cylinder is indicated by a double-headed arrow labeled L_1 . A shorter double-headed arrow labeled L_2 indicates the length of the inner piston rod assembly.

3.3 Eddy Current Damper

Eddy Currents are induced electric currents when a conductor is exposed to a changing magnetic field. The induced currents can be produced either by movement of the conductor in a static magnetic field or a static conductor with varying magnetic field strength. The directions of the induced currents are in a way that generates a magnetic field that opposes the change in magnetic field. This generates a repulsive force that is proportional to the relative velocity of the field and the conductor behaving much like a viscous damper. It must be noted that there is no physical contact between the magnet and the conductor thus no tear and wear of material. Eddy currents have other application such as material separator, metal identification, non-destructive test method for metal and induction heating.

3.3.1 Strength of Eddy Current

The strength of eddy currents or in better terms the force of the magnetic field produced by eddy currents depends on a number of factor; 1. the magnitude of change in magnetic field strength and the strength of the magnetic field within the metal. This depends on the size, strength of the permanent magnet, position of magnet relative to the metal part. 2. The shape, thickness, geometry and type of metal. Thicker pipes and material with higher conductivity generates more braking force. 3. The speed of the magnet or conductor relative to each other. The larger the relative velocity, the larger the force is being produced up to a certain point. Based on the hybrid damper in figure 3.6, there are two components that contribute to the eddy current force; the linear motion and also rotating motion. The basic force is equation is as following:

$$J_i = \sigma \cdot (E + v \times B) \quad (3.16)$$

$$J_i = \sigma(v \times B) \quad (3.17)$$

$$F_B = J_i \times B \quad (3.18)$$

where

J_i = induced current density, A/m²

σ = material electrical conductivity, S/m

v = velocity, m/s

B = magnetic field strength, W/m²

E = Electric Field, N/C

F_B = Lorentz Force, N

3.3.2 Eddy Current Damping Coefficient

Since there is no source or sink of electric currents, there is no electric field produced ($E = 0$) thus equation (3.16) is written as equation (3.17). From equation (3.17) and

(3.18) it can be seen that, to increase the damping force of the damper, the design of the damper will need to use a material with high conductivity and a permanent magnet that can produce strong magnetic field. Besides that, the position of the magnet and the geometry or shape of the design it very important as it affect the magnetic field strength, B. The velocity, v is not a design parameter since it depends on from the road excitation. Equation (3.19) is used to calculate the damping coefficient generated by the eddy current.

$$C_{\text{eddy}} = \int_V \sigma B_r^2 dV \quad (3.19)$$

where,

V = conductor volume, m³

σ = material electrical conductivity, S/m

B_r = radial magnetic flux density, W/m²

3.3.3 Magnet Array Configuration

The permanent magnets are placed on top of each other to form an array of magnets. The ring magnets are used which allows a shaft to go through all the magnets and hold them together and allow for ways to install the damper onto a vehicle. There are a few ways to place and position the magnets together which produces different results (strength of flux density) as shown in figure 4.3 (source from Ebrahimi 2009). The results are in table 4.1(source from Ebrahimi 2009). The arrows show the magnetic field direction.

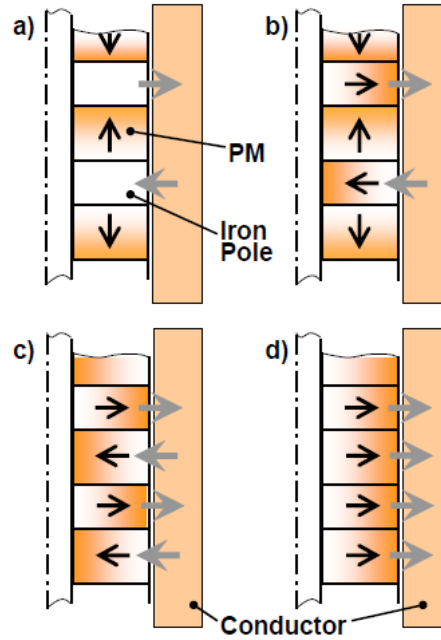


Figure 3.7: Different Permanent Magnet Configuration. a) Axially, b) axially and radially, c) radially (inward and outward), and d) radially(outward) magnetized Permanent Magnets

Table 3.3: Comparison of different Permanent Magnet Configuration

Configuration	(a)	(b)	(c)	(d)
Max(B_r) [T]	2.087	1.627	1.315	0.685
Max(B_r) in the gap[T]	0.68	0.81	0.43	0.18
Damping Coefficient (C) [Ns/m]	52.47	82.46	19.86	3.9

From table 3.3, we can see that configuration (b) in figure 3.7 is able to produce the highest damping coefficient. In fact, the configuration (b) is known as Halbach array which concentrates the magnetic field on one side of the array. Configuration (a) is chosen as part of the design as it uses less magnet material.

3.3.4 Eddy Current Damping Force

For the hybrid eddy current damper, the velocity can be written as equation (3.20). The magnetic flux can be written as equation (3.21). Substituting equation (3.20) and

equation (3.21) into equation (3.17) becomes equation (3.22) which is the induced current density.

$$\mathbf{v} = \omega y \mathbf{i} - \omega x \mathbf{j} + v_z \mathbf{k} \quad (3.20)$$

$$\mathbf{B} = B_x \mathbf{i} + B_y \mathbf{j} + B_z \mathbf{k} \quad (3.21)$$

The current density will be as following:

$$\mathbf{J}_i = \sigma(\mathbf{v} \times \mathbf{B}) = \sigma \begin{bmatrix} (-\omega x B_z - v_z B_y) \mathbf{i} \\ + (v_z B_x - \omega y B_z) \mathbf{j} \\ + (\omega y B_y + \omega x B_x) \mathbf{k} \end{bmatrix} \quad (3.22)$$

Substituting equation (3.22) into equation (3.18) will give equation (3.23) which is the total damping force.

$$\mathbf{F}_B = \sigma \begin{pmatrix} (v_z B_x B_z - \omega x B_x B_y - \omega y (B_y^2 + B_z^2)) \mathbf{i} + \\ (\omega y B_x B_y + v_z B_y B_z + \omega x (B_x^2 + B_z^2)) \mathbf{j} + \\ (\omega y B_x B_z - \omega x B_y B_z - v_z (B_x^2 + B_y^2)) \mathbf{k} \end{pmatrix} \quad (3.23)$$

Equation (3.23) can be written as equation (3.24). Right hand side component of equation (3.24) is in fact the linear Lorentz force, F_L . The left hand side of equation (3.24) is the damping force generated from the rotating magnet, F_R as written in equation (3.25). The total damping force generated is F_B , equation (3.26). Equation (3.27) is the resistive torque cause by the rotating magnet.

$$\mathbf{F}_B = \sigma \begin{pmatrix} (-\omega x B_x B_y - \omega y (B_y^2 + B_z^2)) \mathbf{i} + \\ (\omega y B_x B_y + \omega x (B_x^2 + B_z^2)) \mathbf{j} + \\ (\omega y B_x B_z - \omega x B_y B_z) \mathbf{k} \end{pmatrix} + \sigma \begin{pmatrix} (v_z B_x B_z) \mathbf{i} + \\ (v_z B_y B_z) \mathbf{j} + \\ (-v_z (B_x^2 + B_y^2)) \mathbf{k} \end{pmatrix} \quad (3.24)$$

$$F_R = \sigma \begin{pmatrix} (-\omega x B_x B_y - \omega y (B_y^2 + B_z^2)) i + \\ (\omega y B_x B_y + \omega x (B_x^2 + B_z^2)) j + \\ (\omega y B_x B_z - \omega x B_y B_z) k \end{pmatrix} \quad (3.25)$$

$$F_B = F_R + F_L \quad (3.26)$$

$$T_{mg} = F_R * R \quad (3.27)$$

According to Ebrahimi (2009), the vertical component of the magnetic flux, B_z does not contribute to the generation of eddy current for vertical motion and only the radial component of the magnetic flux does. Since the magnet is placed in such a way that only the radial component of the magnetic flux is in use, the eddy current caused by the rotational motion will only be contributed by radial component. Hence equation (3.24), is now equation (3.28) with $B_z = 0$. By comparing equation (3.20) and equation (3.28), it can be seen that, the force is in the opposite direction from the velocity.

$$F_B = \sigma \begin{pmatrix} (-\omega x B_x B_y - \omega y B_y^2) i + \\ (\omega y B_x B_y + \omega x B_x^2) j + \\ (-v_z (B_x^2 + B_y^2)) k \end{pmatrix} \quad (3.28)$$

3.4 Sizing of magnet

To determine the dimension of the eddy current damper, firstly the size of magnets needs to be determined. The size of the magnet is determined via magnetic circuit analysis. Magnetic circuit analysis is used to determine the design parameters and the damper performance. Figure 3.8 shows the 2d half lumped model of the proposed eddy current damper and the flow of magnetic flux. The magnetic circuit is assumed to have no leakage flux and no fringing magnetic fields. The analysis is performed

for one pole pair only. Figure 3.9 shows the equivalent circuit of the lumped model in figure 3.8.

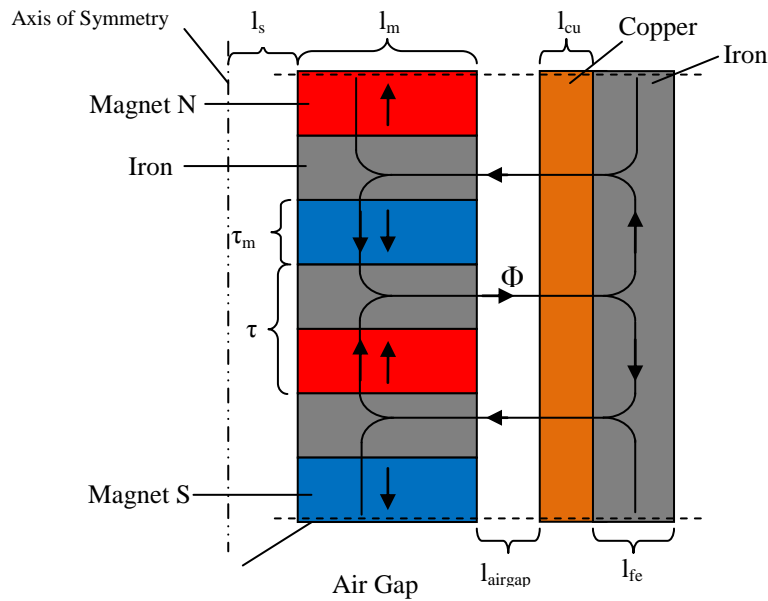


Figure 3.8: Half lumped model of Eddy Current Damper

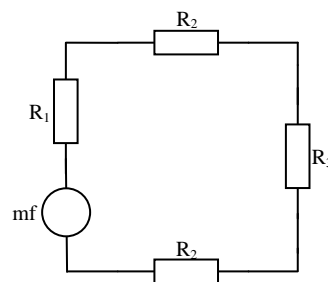


Figure 3.9: Equivalent circuit for one pole pair of the lumped model.

R_1 , R_2 and R_3 are reluctance of the magnetic circuit and are grouped together based on same cross-sectional area. mf is the magneto force produced by the permanent magnet.

$$H_m L_m = \Phi (R_1 + 2R_2 + R_3) \tag{3.29}$$

$$R_1 = \frac{(\Gamma - T_m)}{\mu_i \pi (l_m^2 + 2l_m l_s)} \tag{3.30}$$

$$R_2 = \frac{1}{2\pi(l_s + l_m)(T - T_m)} \left[\frac{l_m}{2\mu_i} + \frac{l_g}{\mu_0} + \frac{l_{cu}}{\mu_{cu}} + \frac{l_{fe}}{2\mu_i} \right] \quad (3.31)$$

$$R_3 = \frac{1}{\pi\{(l_s + l_m + l_g + l_{cu} + l_{fe})^2 - (l_s + l_m + l_g + l_{cu})^2\}} \left[\frac{T}{\mu_i} \right] \quad (3.32)$$

where,

T = Thickness of magnet and pole, mm

T_m = Thickness of magnet, mm

l_m = length of magnet core, mm

l_s = length of air core, mm

l_g = length of air gap, mm

l_{cu} = length of copper, mm

l_{fe} = length of iron, mm

μ_i = absolute permeability of iron, Hm^{-1}

μ_0 = relative permeability of free space, Hm^{-1}

μ_{cu} = absolute permeability of copper, Hm^{-1}

3.4.1 Magnet Size

To produce a maximum energy density of magnetic field into the air gap, an operating point on the hysteresis curve that makes the energy product $B_m H_m$ maximum is used. Besides this, it is important to take note of the operating temperature. The maximum operating temperature and operating point depends on the shape of the magnet. The measure of this shape is called the Permeance of Coefficient.

$$P_c = \left(\frac{L_m}{L_g} \right) \cdot \left(\frac{A_g}{A_m} \right) \quad (3.33)$$

where

L_m = length of magnet (parallel to the flow of flux), m

L_g = Length of air gap (parallel to the flow of flux), m

A_g = cross-sectional area of the air gap perpendicular to the flux path, m^2

A_m = the cross-sectional area of the magnet, m^2

Based on figure 3.10, Neodymium Iron Boron (NdFeB) is chosen as the magnet material due to its highest energy product, high coercivity force, and reasonable relative cost.

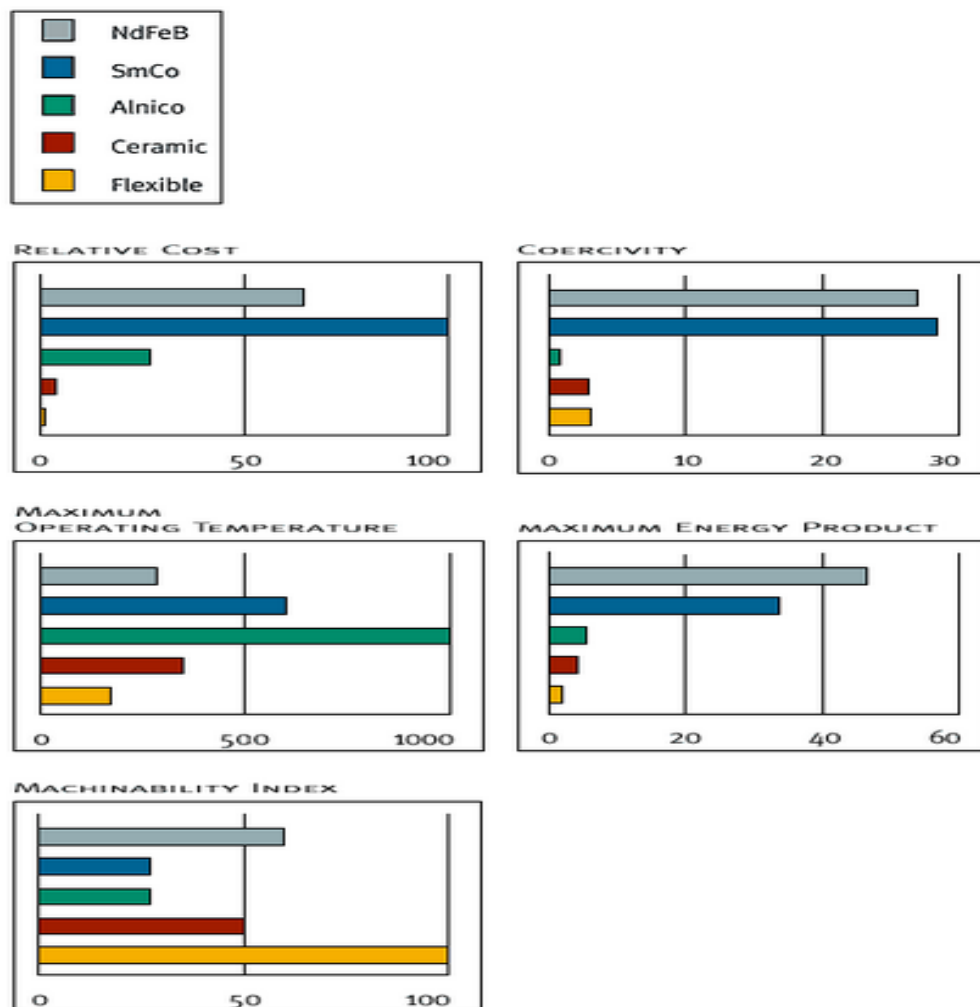


Figure 3.10: Quick Comparison Chart of 4 types of magnets (2000 Magnet Sales & Manufacturing Company. Inc.)

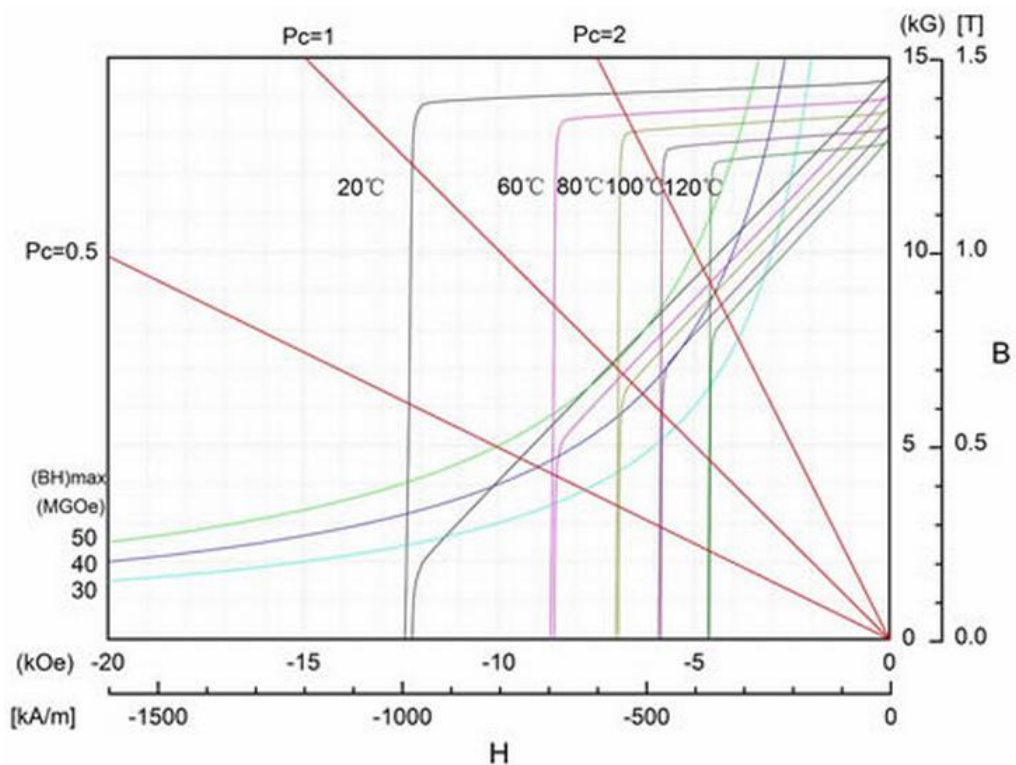


Figure 3.11: Demagnetization Curves at Different Temperature for N52 grade magnet. (2010 – 2015 THMAG Tianhe Advanced)

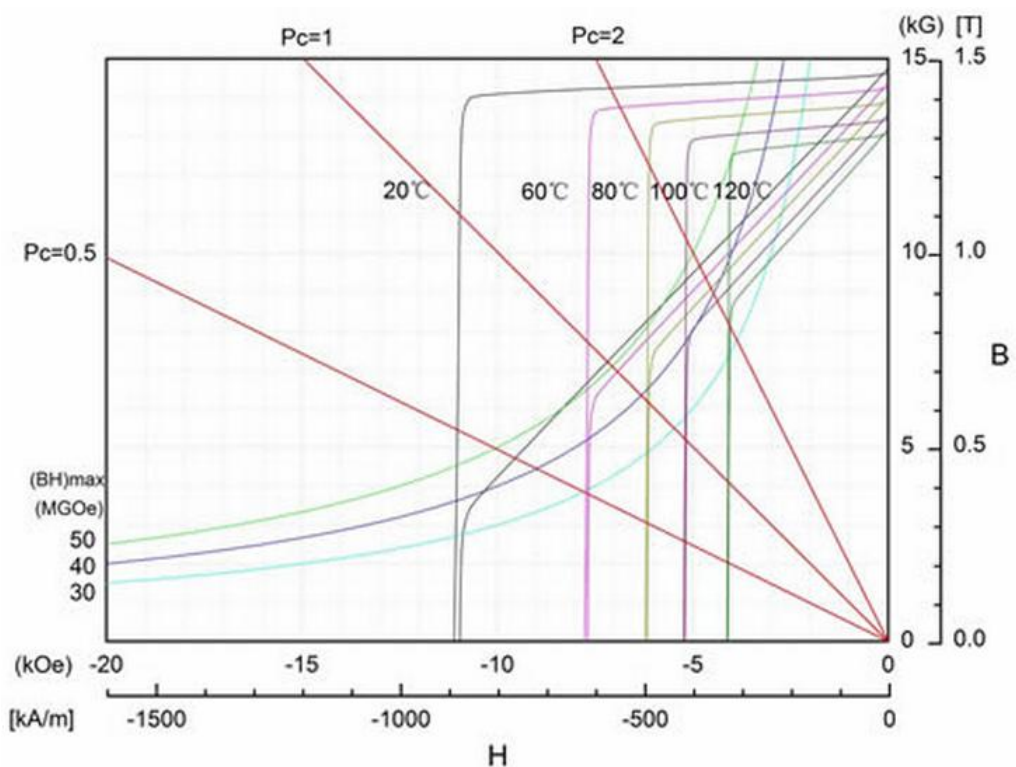


Figure 3.12: Demagnetization Curves at Different Temperature for N54 grade magnet. (2010 – 2015 THMAG Tianhe Advanced)

Table 3.4: Magnetic Characteristic of N52 and N54 Grade magnet(2010 – 2015 THMAG Tianhe Advanced)

Item	Unit	Grade N52	Grade N54
Residual flux density, Br	[T]	1.42-1.48	1.45-1.51
Coercive force, Hcb	[kA/m]	≥836	≥836
Intrinsic coercive force, Hcj	[kA/m]	≥876	≥876
Maximum energy product (BH) _{max}	[kJ/m ³]	390-422	406-438

From table 3.4, the N54 grade magnet has higher energy product compared to N52 grade magnet but N52 magnet can operate at a slightly higher temperature. Based on the load line, $P_c = 1.0$ from figure 3.11 and 3.12, the operating point at 80 °C for N52 magnet is before ‘drop’ or ‘knee’ while for N54 is after the ‘knee’. This shows that for N52 magnets with permeance of coefficient of 1.0, is able to operate at 80 °C without loss of magnetization which is a better choice compared to N54 magnets of the same size and shape. Besides, at P_c equals 1.0, N52 operates at BH_{max} at 20 °C. Based on figure (3.8), the variable in equation (3.33) is now equation (3.34).

$$P_c = \left(\frac{T_m}{2l_g} \right) \cdot \left(\frac{2\pi(l_s + l_m)(T - T_m)}{\pi((l_s + l_m)^2 - l_s^2)} \right) = \left(\frac{T_m}{l_g} \right) \cdot \left(\frac{(l_s + l_m)(k \cdot T_m - T_m)}{l_m^2 + 2l_m l_s} \right) \quad (3.34)$$

where,

$T = k \cdot T_m$, k ratio.

3.5 Sizing of Copper & Iron Cylinder

The size of thickness of the copper cylinder will approximated using eddy current penetration. The sizing of copper cylinder will affect the sizing of the magnet. A balance between magnet size and damping force is necessary for the overall size of the damper. Matlab is used to compute equation (3.35) and (3.36). Copper is used as the material for the computation. For the outer part which is the iron cylinder, Comsol 4.2 multiphysics will be used to determine the minimum size required.

$$\delta = \frac{1}{\sqrt{\pi f \mu_{\text{cu}} \sigma}} \quad (3.35)$$

$$J = J_S e^{-\frac{d}{\delta}} \quad (3.36)$$

where,

δ = depth of penetration or skin depth, mm

f = frequency of oscillation, Hz

μ_{cu} = absolute permeability of Copper, Hm^{-1}

σ = conductivity of copper, S/m

J = depth current density, A/m^2

J_S = Surface current density, A/m^2

d = depth from the surface, mm

3.6 Energy Regeneration

Energy Regeneration for the damper component is based on induced voltage/current by magnet. Based on the said laws, electricity is generated only if there is, 1) change of magnetic flux, 2) relative velocity between the magnet and the coil. There is no flux change for a permanent magnet thus the only way to generate electricity is through motion. Maximum electricity is generated when the coil is perpendicular to the magnetic flux lines. The coils should be placed in a way that is always perpendicular to the magnetic flux and closes to the maximum flux generated. To generate the maximum electricity from any given motion, the coils should be placed in groups that take account of the direction of magnetic flux flow from the magnet array and is able to generate electricity as long as there is relative motion.

$$E_i = Blv \quad (3.37)$$

$$I = \frac{E_i}{R} = \sigma A_w B_r v_z \quad (3.38)$$

$$P = E_i I = \sigma l A_w B_r^2 v_z^2 \quad (3.39)$$

where

E_i = EMF voltage, V

I = maximum induced current(short circuit), A

R = resistance of wire, Ω

σ = electrical conductivity of wire, S/m

A_w = Area of conductor wire, m^2

B_r = radial magnetic flux, T/m^2

v_z = vertical velocity, ms^{-1}

P = power produced, W

Three-phase power generator concept is used for the energy regeneration. Three phase power generator has the advantage of constant power flow and lower losses. Figure 5.13 shows the coil placement inside the eddy current damper. The coils are placed in groups of 4. This is to ensure that the magnetic flux are fully utilised and does not interfere with electric regeneration of other coils during the up down motion of the magnet array. The size of the copper coil used will affect the number of turns of the coil. The smaller the diameter of the wire, the more turns available on the coil thus, more flux is cut which in turn produces higher voltage. Matlab will be used to simulate the power generated. The 35 SWG enamelled copper is used for the coil.

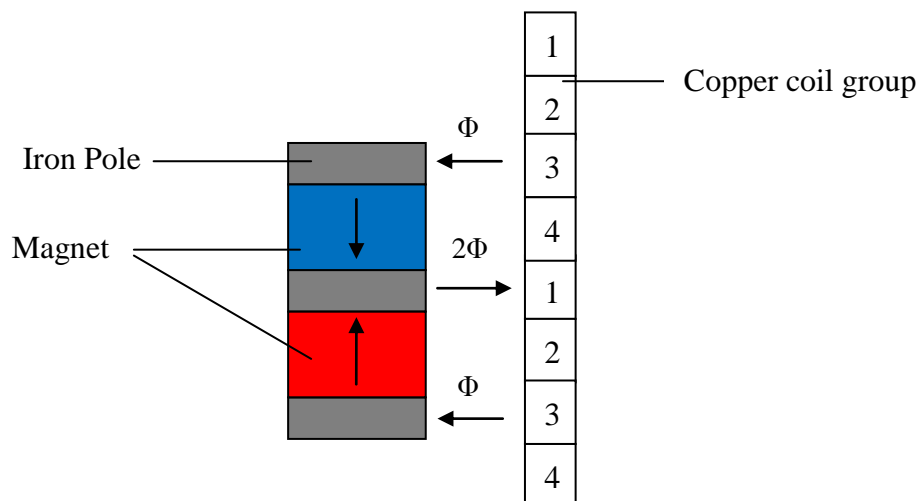


Figure 3.13: Coil placement in the eddy current damper.

CHAPTER 4

RESULTS AND DISCUSSIONS

4.1 Magnet Size

Matlab is used to calculate all the possible value for $P_c = 1$ or close to 1 on equation (3.34). l_s is the diameter of shaft of the ball screw which is set constant to 25mm. The parameter are, l_m , k , T_m and l_g as shown in figure 3.8. The size of the magnet will affect the strength of the magnetic field. It must also be a feasible size so that the overall size of the damper is not too large. Based on table 4.1, the yellow shaded values are taken for the magnet size.

Table 4.1: Different sets of value for $P_C \approx 1.0$

$l_g +$ l_{cu}/mm	l_m /mm	P_C	T /mm	k	T_m /mm	$T - T_m$
5	17.0	1.0118	23.8	1.7	14.0	9.8
	18.0	1.1017	25.2	1.8	14.0	11.2
	16.0	1.0483	24.0	1.6	15.0	9
	17.0	1.1615	25.5	1.7	15.0	10.5
	15.0	1.0503	24.0	1.5	16.0	8
	16.0	1.1927	25.6	1.6	16.0	9.6
	14.0	1.0063	23.8	1.3	17.0	6.8
	15.0	1.1856	25.5	1.5	17.0	8.5
	14.0	1.1282	25.2	1.4	18.0	7.2

	13.0	1.0050	24.7	1.3	19.0	5.7
	13.0	1.1136	26.0	1.3	20.0	6
	12.0	1.0523	27.6	1.2	23.0	4.6
	12.0	1.1458	28.8	1.2	24.0	4.8
10	18.0	1.0146	34.2	1.8	19.0	15.2
	17.0	1.0325	34.0	1.7	20.0	14
	18.0	1.1242	36.0	1.8	20.0	16
	16.0	1.0273	33.6	1.6	21.0	12.6
	17.0	1.1383	35.7	1.7	21.0	14.7
	16.0	1.1275	35.2	1.6	22.0	13.2
	15.0	1.0851	34.5	1.5	23.0	11.5
	14.0	1.0029	33.6	1.4	24.0	9.6
	15.0	1.1815	36.0	1.5	24.0	12
	14.0	1.0882	35.0	1.4	25.0	10
	14.0	1.1770	36.4	1.4	26.0	10.4
	13.0	1.0147	35.1	1.3	27.0	8.1
	13.0	1.0913	36.4	1.3	28.0	8.4
	13.0	1.1706	37.7	1.3	29.0	8.7
15	18.0	1.0792	43.2	1.8	24.0	19.2
	17.0	1.0755	42.5	1.7	25.0	17.5
	18.0	1.1710	45.0	1.8	25.0	20
	16.0	1.0498	41.6	1.6	26.0	15.6
	17.0	1.1633	44.2	1.7	26.0	18.2
	16.0	1.1322	43.2	1.6	27.0	16.2
	15.0	1.0721	42.0	1.5	28.0	14
	15.0	1.1501	43.5	1.5	29.0	14.5
	14.0	1.0446	42.0	1.4	30.0	12

4.2 Sizing of Copper Cylinder

The result in figure 4.1 is based on equation (3.35) and figure 4.2 is based on equation (3.36) on a copper cylinder. It can be seen that, the higher the oscillation the

shorter the depth of penetration in the copper. As the frequency of oscillation increases, the current density in the copper decreases. The current density also decreases in depth.

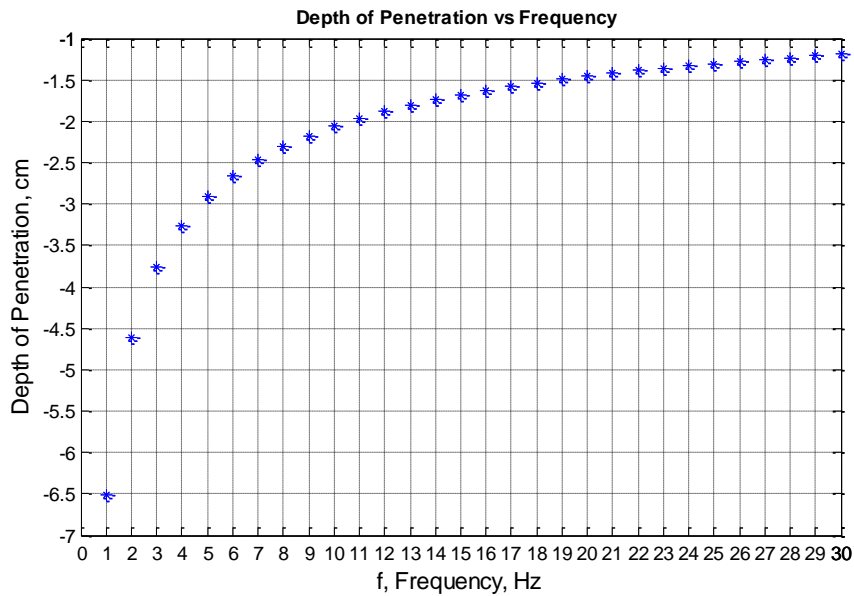


Figure 4.1: Relation between Eddy Current Penetration and Oscillating Frequency

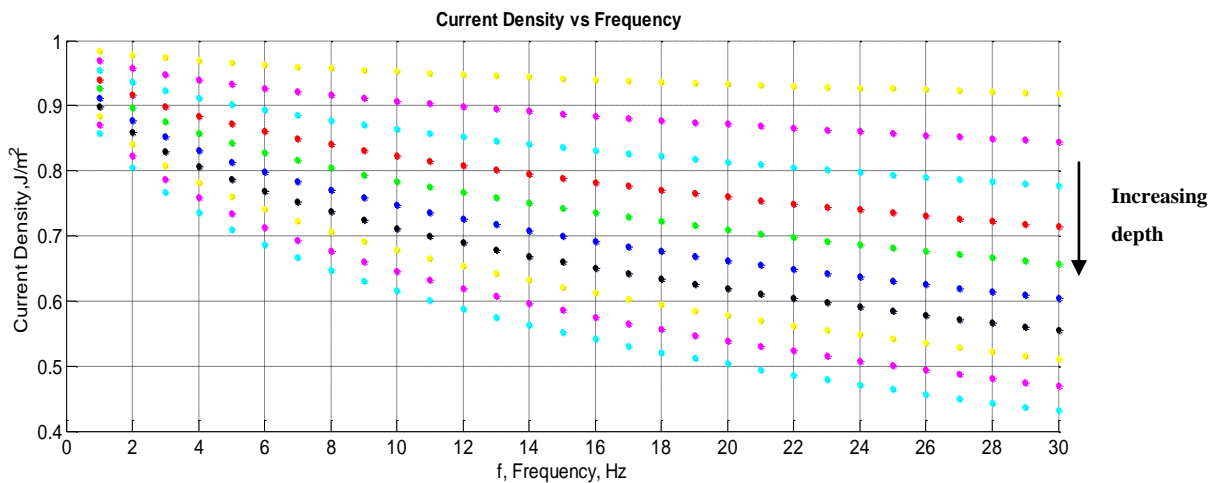


Figure 4.2: Relation between Current Density and Oscillating Frequency

Depending on the frequency of the oscillation of the magnet array, the copper cylinder does not always need to be large. Comsol 4.2 is used to simulate and decide the minimum copper thickness using the magnet size in table 4.1. Figure 4.3 shows one of the results for simulating linear motion of the eddy current damper to determine the minimum width. The results of the force is shown in figure 4.4

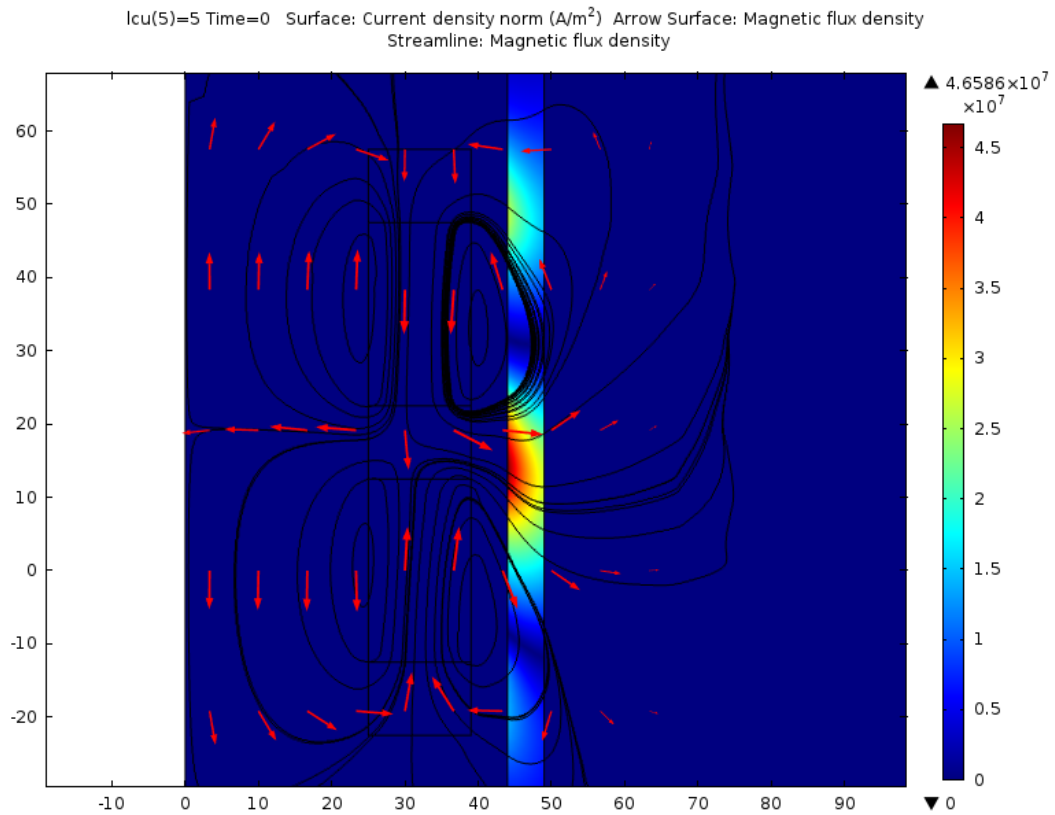


Figure 4.3: 2d View of Eddy Current simulation to determine the copper width (linear motion)

As seen from figure 4.4, the thickness of the copper will affect the Lorentz force to a certain extent. Generally, the higher the velocity of the magnet, the larger the force will be generated. According to figure 4.4, the thickness of the copper will affect the force generated at different speeds. For speeds of 5 m/s the force generated is at peak when thickness of copper is 5mm. Due to size constraint, 5mm will be chosen.

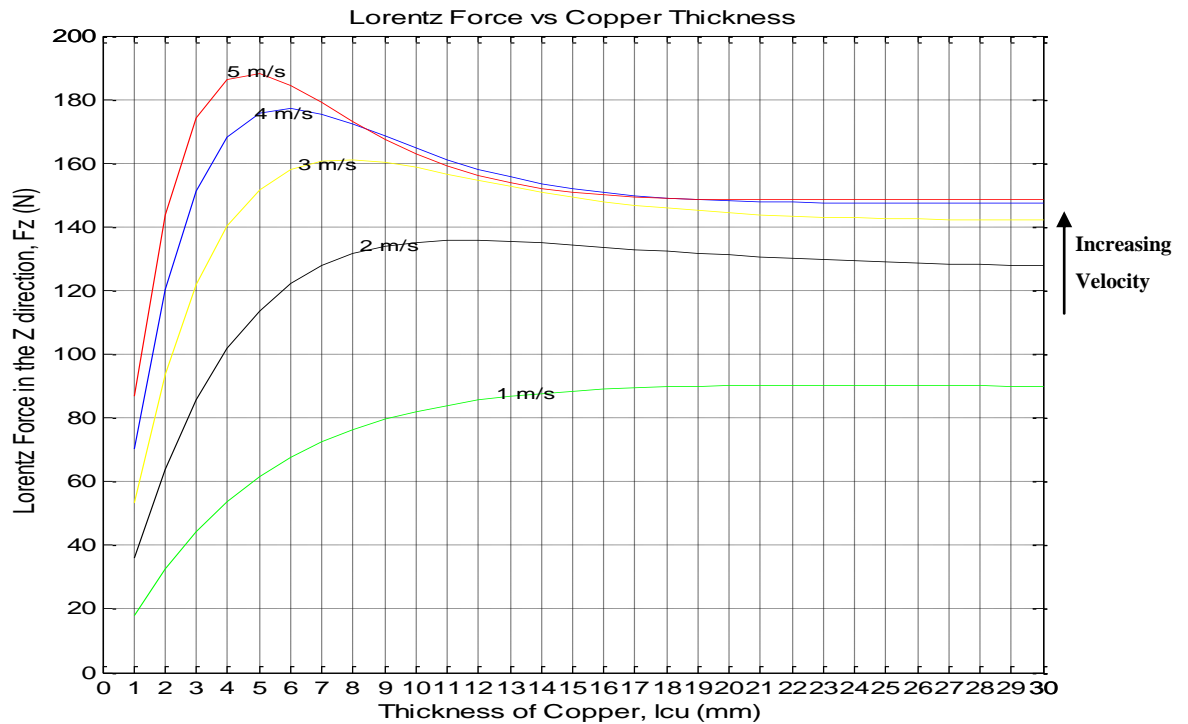


Figure 4.4: Relation between Lorentz Force and Copper Thickness with air gap of 5mm with magnet at 7.5T (linear motion)

4.3 Sizing of Iron Cylinder

From figure 4.4 and figure 4.6, we can see the improvement in force by adding an outer iron tube. The force is much more constant for the copper and iron tube compared to the purely copper tube only. The Iron Core thickness between 1mm to 3mm is sufficient to increase the force of the damper. The force generated is highest at speeds of 4m/s. The force is almost similar for speeds of 3m/s and 5m/s. Table 4.2 is acquired based on figure 3.4 and equation (3.30) to equation (3.32) to compare the differences. The simulation result in figure 4.5 is almost similar with figure 4.4 but with added iron beside the copper.

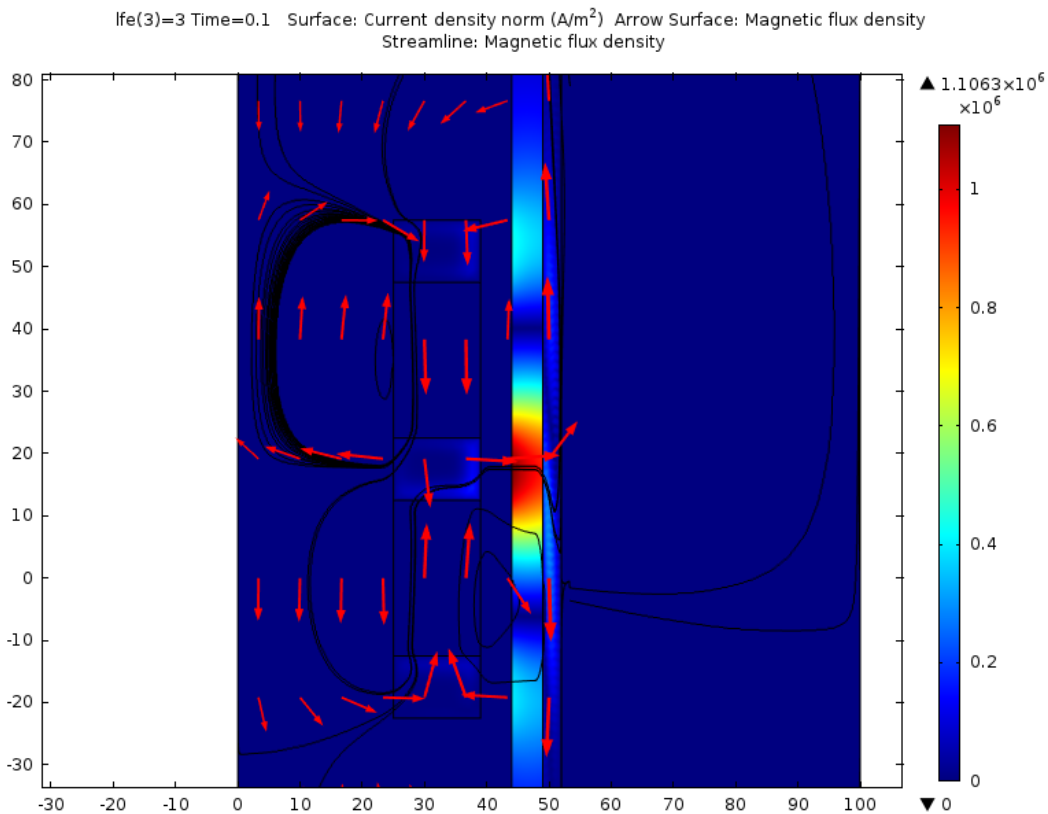


Figure 4.5: 2d View of Eddy Current simulation to determine the iron width (linear)

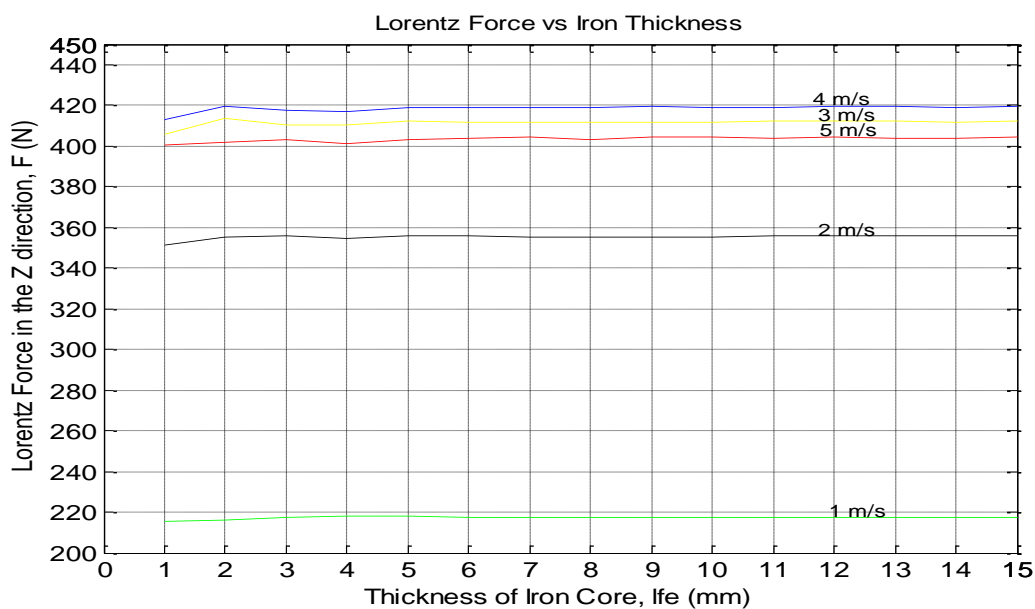


Figure 4.6: Relation between Lorentz Force and Iron Thickness (with air gap of 5mm, Copper thickness of 5mm with magnet at 7.5T)

Figure 4.7 shows the velocity profile of different iron width. It can be seen that as the width increases, so does the time taken for the damper to reach zero velocity.

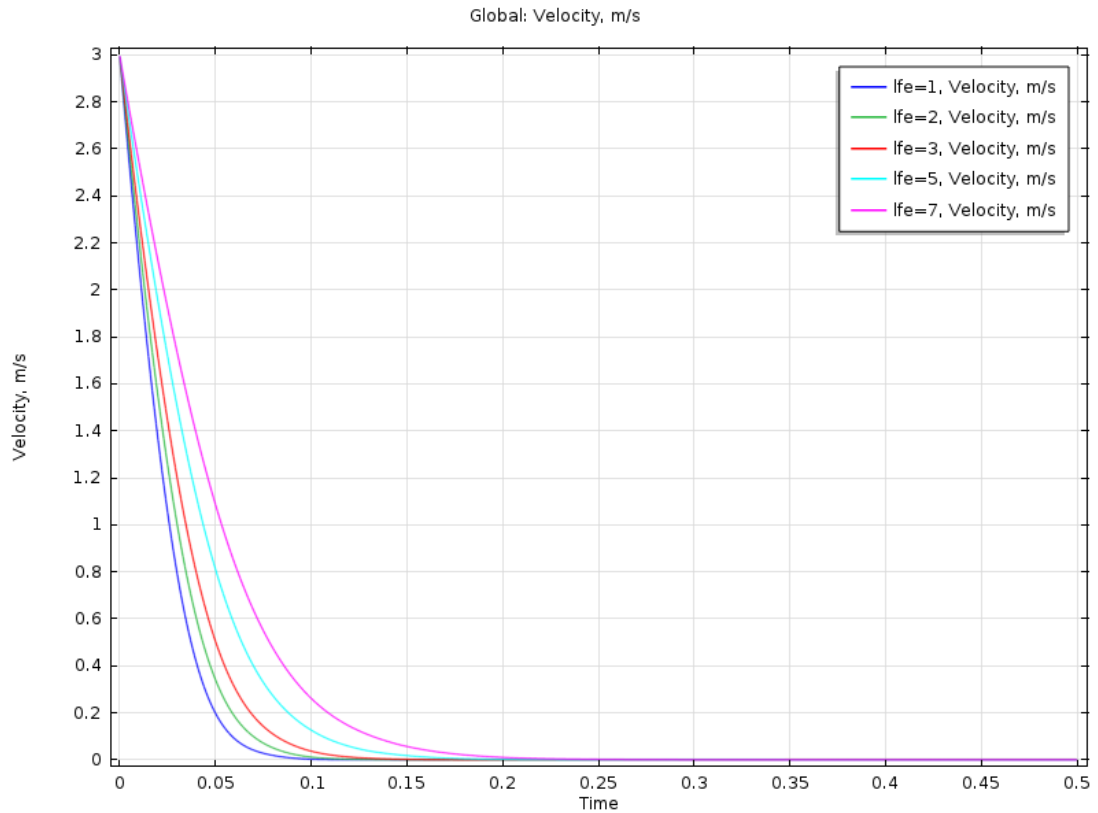


Figure 4.7: Velocity profile of damper with copper width, $l_{cu} = 5\text{mm}$ and variable iron width, l_{fe} (mm)

Table 4.2: Reluctance of the magnetic circuit with different iron thickness

l_{fe} (mm)	1 (H^{-1})	2 (H^{-1})	3 (H^{-1})
R1	8.88026E-07	8.88026E-07	8.88026E-07
R2	0.004081336	0.004081387	0.004081438
R3	2.81298E-05	1.39243E-05	9.19093E-06
Total Reluctance	0.004110354	0.004096199	0.004091517
Percentage of difference (%)	0.344363187		0.11430894

As seen in table 4.2, as the thickness of the iron core increases, the total reluctance decreases. The percentage of decrease in reluctance as the thickness

increases is very small with the highest decrease is between $l_{fe} = 1$ and $l_{fe} = 3$ is about 0.46%. The decrease in reluctance is very small thus, 1 mm is chosen for the thickness of the iron core based on figure 4.6 & figure 4.7.

4.3.1 Energy Regeneration

The result shown in figure 4.8 and figure 4.9 are simulated based on the position of the magnet, the velocity profile of the oscillation and length of the coil cut by the flux. An average radial magnetic flux from figure 3.13 is taken to be 0.5 T for the simulation. Only one coil is used for this simulation as the rest of the result can be multiply from there on. The resistant is assumed to be a combination group of 50 coils. By comparing figure 4.8 and figure 4.9, at higher frequency, more power is generated per half a second. The coding is shown in Appendix B.

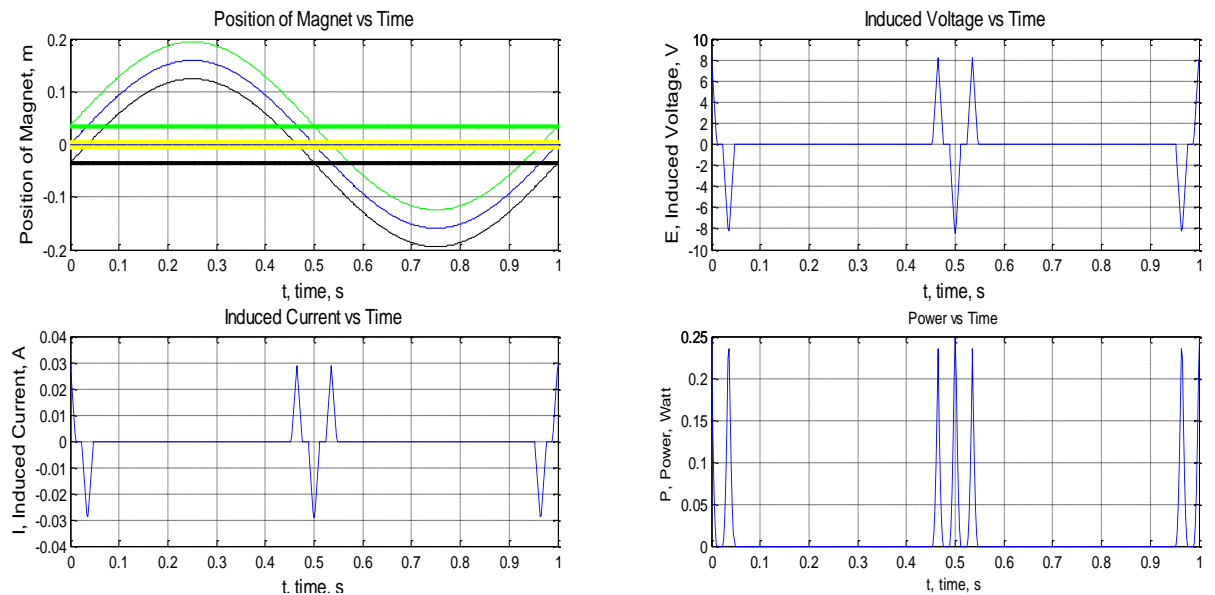


Figure 4.8: Combination of graph for Oscillation Frequency = 1 Hz, initial velocity = 1m/s

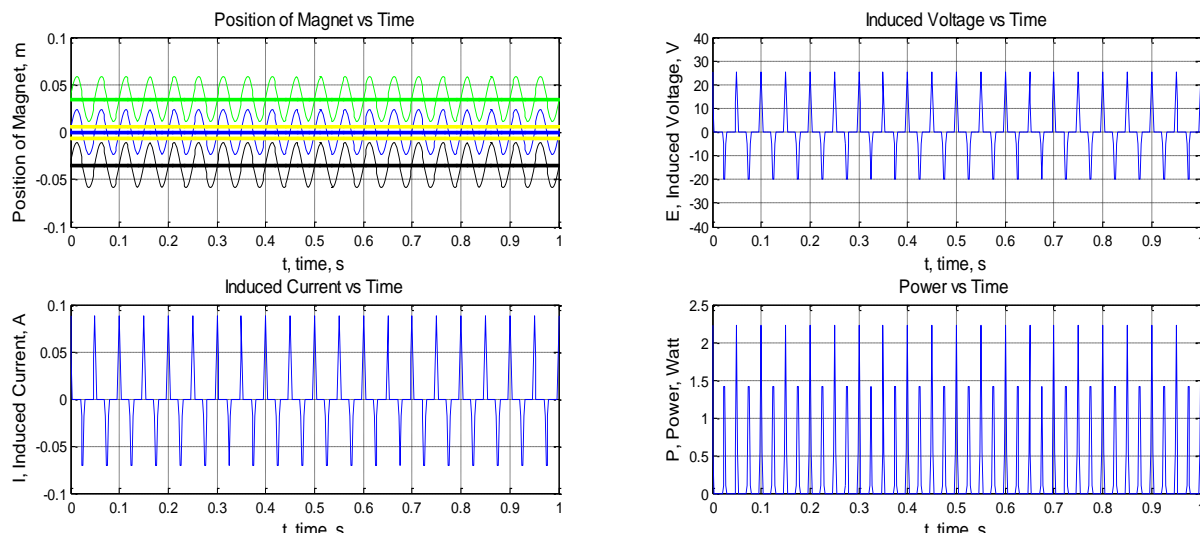


Figure 4.9: Combination of graph for Oscillation Frequency = 20 Hz, initial velocity = 3m/s

From figure 4.8, the oscillation is set at 1 Hz with maximum speed of 1 m/s. It can be seen that all three magnet passes through the coil. The maximum voltage generated is about 8 volts. Depending on the resistance of the wire, the current value will be different so does the power output in which this case has a maximum value of 0.23 watts. From figure 4.9, the oscillation is set to 20 Hz with maximum speed of 3 m/s. It can be seen that only one magnet passes through the coil but the voltage generated is about 25 volts. Likewise, the power generation depends on the current which depends on the resistant of the wire, which this case the maximum value is 2.3 watts. Based on this two results, we can see that the amplitude of oscillation will determine the output waveform while the velocity will determine the magnitude of the output: the higher the velocity the higher the voltage produced.

CHAPTER 5

CONCLUSION AND RECOMMENDATIONS

5.1 Hybrid Shock Absorber

Based on the result shown above, the hybrid damper has the following dimension as shown in table 5.1.

Table 5.1: Summary of the Eddy Current Damper for hybrid damper

Outer Diameter, cm	10
height of magnetic array, cm	8
height of Eddy Current damper, cm	40

Based on table 5.1, the outer diameter is 10 cm which is very large. It is due to the fact that the shaft is assumed to have a diameter of 5 cm. The shaft size is not chosen by the author in this paper. It is shown in the result that, the damper is able to provide addition damping to for the ball screw suspension system. The power regeneration is shown to be able to produce a small amount of power in which with the right energy storage is able to contribute to prolong the distance travelled by an EV.

5.2 Recommendation

This is just a brief conceptual design of a new hybrid shock absorber and more studies are required to improve the system. The first problem to tackle is the size of

the damper itself. The shaft of the damper must be made out of non magnetic material and also a study must be conducted to know the minimum sized required for the shaft. By reducing the shaft diameter to half, we can easily reduce the size of the damper to half. For the magnet array, to increase the force, a Halbach configuration can be considered. There must also be limiter and stopper to avoid the knocking of magnetic array on the ceiling and bottom of the shock absorber.

REFERENCES

- Ebrahimi, B., Khamesee, M. B., & Golnaraghi, F. (2009). Eddy current damper feasibility in automobile suspension: modeling, simulation and testing. *Smart Materials and Structures*, 18(1), 015017.
- Ebrahimi, B. (2009). *Development of hybrid electromagnetic dampers for vehicle suspension systems* (Doctoral dissertation, University of Waterloo).
- Lin, X., & Xuexun, G. (2010, May). Hydraulic Transmission Electromagnetic Energy-Regenerative Active Suspension and Its Working Principle. In *Intelligent Systems and Applications (ISA), 2010 2nd International Workshop on* (pp. 1-5). IEEE.
- Liu, S., Wei, H., & Wang, W. (2011, August). Investigation on some key issues of regenerative damper with rotary motor for automobile suspension. In *Electronic and Mechanical Engineering and Information Technology (EMEIT), 2011 International Conference on* (Vol. 3, pp. 1435-1439). IEEE.
- Montazeri-Gh, M., & Kaviani-pour, O. (2012). Investigation of the passive electromagnetic damper. *Acta Mechanica*, 223(12), 2633-2646.
- Oprea, R. A., Mihailescu, M., Chirila, A. I., & Deaconu, I. D. (2012, May). Design and efficiency of linear electromagnetic shock absorbers. In *Optimization of Electrical and Electronic Equipment (OPTIM), 2012 13th International Conference on* (pp. 630-634). IEEE.
- Paz, O. D. (2004). *The Department of Electrical and Computer Engineering* (Doctoral dissertation, Universidad del Zulia).
- Zhang, Y., Huang, K., Yu, F., Gu, Y., & Li, D. (2007, December). Experimental verification of energy-regenerative feasibility for an automotive electrical suspension system. In *Vehicular Electronics and Safety, 2007. ICVES. IEEE International Conference on* (pp. 1-5). IEEE.
- Zuo, L., Scully, B., Shestani, J., & Zhou, Y. (2010). Design and characterization of an electromagnetic energy harvester for vehicle suspensions. *Smart Materials and Structures*, 19(4), 045003.

- Zhang, Y., Huang, K., Yu, F., Gu, Y., & Li, D. (2007, December). Experimental verification of energy-regenerative feasibility for an automotive electrical suspension system. In *Vehicular Electronics and Safety, 2007. ICVES. IEEE International Conference on* (pp. 1-5). IEEE.
- Liu, S., Wei, H., & Wang, W. (2011, August). Investigation on some key issues of regenerative damper with rotary motor for automobile suspension. In *Electronic and Mechanical Engineering and Information Technology (EMEIT), 2011 International Conference on* (Vol. 3, pp. 1435-1439). IEEE.
- Montazeri-Gh, M., & Kavianipour, O. (2012). Investigation of the passive electromagnetic damper. *Acta Mechanica*, 223(12), 2633-2646.
- Wu Zhengguang, Cao Yu. Brief Introduction to Structure and Principle of Electromagnetic Shock Absorber. *Motor Technology*, 2007,8 pp 56 -59
- Zhang Yong-chao, Yu Fan, Gu Yong, Zhen Xue-chun. Isolation and Energy-regenerative Performance Experimental Verification of Automotive Electrical Suspension. *Journal of Shanghai JiaoTong University*, 2008.6 Vol.42, No.6, pp 874-877
- He Ren, Chen Shian, Lu Senlin. *A Permanent Magnetic Energyregenerative Suspension*. China: ZL200520072480.9
- Chen Shia, He Ren, Lu Senlin. Operation Theory and Structure Evaluation of Reclaiming Energy Suspension. *Transactions of the Chinese Society for Agricultural Machinery*, 2006.5, Vol.37, No5, pp 5-9

APPENDICES

APPENDIX A: Computer Programme Listing

Matlab coding for results in figure 4.8 and figure 4.9.

```

%Paramter%
z0 = 0;           %[m]location of coil 3
B0 = 0.5;        %[T]average magnetic flux density
v0 = 3;          %[m/s] initial velocity
f = 20;          %[Hz]frequency of oscillation
w = 2*pi*f;
Tm = 0.025;      %[m] magnet thickness/height
Tp = 0.010;      %[m] thickness/height of iron pole
T = Tm + Tp;     %[m]
Tc = 0.012;      %[m] height of coil

Rw = 0.00015;    %[m]Radius of wire
Rc = 0.040;      %[m] radius of coil

r = 0.5657;      % ohm/m @ 20
                 degree C
L = 50*((2*Rw)^2 + (2*pi*(Rw+Rc))^2)^0.5*(Tc/(2*Rw)); %Length of
wire along the coil
R = r*L;         %total
                 resistance of coil

t = 0:0.002:1;   %time, s

for i = 1:501

    z(i) = z0 + (v0/w)*sin(w*t(i));

    v(i) = v0*cos(w*t(i));

    z2(i) = -T + z(i);

    z3(i) = z(i) + T;

    if(((z(i)+Tp/2)>Tc/2)&&((z(i)-Tp/2)<Tc/2))||(((z(i)-Tp/2)<-
Tc/2)&&((z(i)+Tp/2)>-Tc/2))||(((z(i)+Tp/2)<=Tc/2)&&((z(i)-Tp/2)>=-
Tc/2))) %coil3

```



```

B = 2*B0;

if (z(i)+Tp/2)>Tc/2

    h(i)= (Tc/2)-(z(i)-Tp/2); %flux between magnetic and coil
    N(i) = (h(i)/(2*Rw));      %Number of turn of coil
    l(i) = (((2*Rw)^2 + (2*pi*(Rw+Rc))^2)^0.5)*N(i);
    E(i) = B*v(i)*l(i);
    I(i) = E(i)/R;
    P(i) = E(i)*I(i);

elseif (z(i)-Tp/2)<-Tc/2

    h(i) = (Tc/2)-(-z(i)-Tp/2);
    N(i) = (h(i)/(2*Rw));      %Number of turn of coil
    l(i) = (((2*Rw)^2 + (2*pi*(Rw+Rc))^2)^0.5)*N(i);
    E(i) = B*v(i)*l(i);
    I(i) = E(i)/R;
    P(i) = E(i)*I(i);

else

    h(i) = Tp;
    N(i) = (h(i)/(2*Rw));      %Number of turn of coil
    l(i) = (((2*Rw)^2 + (2*pi*(Rw+Rc))^2)^0.5)*N(i);
    E(i) = B*v(i)*l(i);
    I(i) = E(i)/R;
    P(i) = E(i)*I(i);

end

end

if(((z2(i)+Tp/2)>Tc/2)&&((z2(i)-Tp/2)<Tc/2))||(((z2(i)-Tp/2)<-
Tc/2)&&((z2(i)+Tp/2)>-Tc/2))||(((z2(i)+Tp/2)<=Tc/2)&&((z2(i)-
Tp/2)>=-Tc/2)))

    B = -B0;

    if (z2(i)+Tp/2)>Tc/2

        h(i)= (Tc/2)-(z2(i)-Tp/2); %flux between
magnetic and coil
coil
        N(i) = (h(i)/(2*Rw));      %Number of turn of
coil
        l(i) = (((2*Rw)^2 + (2*pi*(Rw+Rc))^2)^0.5)*N(i);
        E(i) = 2*B*v(i)*l(i);
        I(i) = E(i)/R;
        P(i) = E(i)*I(i);

    elseif (z2(i)-Tp/2)<-Tc/2

        h(i) = (Tc/2)-(-z2(i)-Tp/2);
coil
        N(i) = (h(i)/(2*Rw));      %Number of turn of
coil
        l(i) = (((2*Rw)^2 + (2*pi*(Rw+Rc))^2)^0.5)*N(i);
        E(i) = 2*B*v(i)*l(i);
        I(i) = E(i)/R;
        P(i) = E(i)*I(i);

```

```

else
    h(i) = Tp;
    N(i) = (h(i)/(2*Rw));           %Number of turn of
coil
    l(i) = (((2*Rw)^2 +
(2*pi*(Rw+Rc))^2)^0.5)*N(i);
    E(i) = 2*B*v(i)*l(i);
    I(i) = E(i)/R;
    P(i) = E(i)*I(i);

end

end

if ((z3(i)+Tp/2)>Tc/2)&&((z3(i)-Tp/2)<Tc/2)||((z3(i)-Tp/2)<-
Tc/2)&&((z3(i)+Tp/2)>-Tc/2))||((z3(i)+Tp/2)<=Tc/2)&&((z3(i)-
Tp/2)>=-Tc/2))

    B = -B0;

    if (z3(i)+Tp/2)>Tc/2

        h(i)= (Tc/2)-(z3(i)-Tp/2); %flux between
magnetic and coil
        N(i) = (h(i)/(2*Rw));           %Number of turn of
coil
        l(i) = (((2*Rw)^2 + (2*pi*(Rw+Rc))^2)^0.5)*N(i);
        E(i) = 2*B*v(i)*l(i);
        I(i) = E(i)/R;
        P(i) = E(i)*I(i);

    elseif (z3(i)-Tp/2)<-Tc/2

        h(i) = (Tc/2)-(-z3(i)-Tp/2);
        N(i) = (h(i)/(2*Rw));           %Number of turn of
coil
        l(i) = (((2*Rw)^2 + (2*pi*(Rw+Rc))^2)^0.5)*N(i);
        E(i) = 2*B*v(i)*l(i);
        I(i) = E(i)/R;
        P(i) = E(i)*I(i);

    else
        h(i) = Tp;
        N(i) = (h(i)/(2*Rw));           %Number of turn of
coil
        l(i) = (((2*Rw)^2 +
(2*pi*(Rw+Rc))^2)^0.5)*N(i);
        E(i) = 2*B*v(i)*l(i);
        I(i) = E(i)/R;
        P(i) = E(i)*I(i);

    end

end

end
end

```

```
figure(1);
subplot(2,2,1),plot(t,z,'b');
hold on;
plot(t,z2,'k');
plot(t,z3,'g');
plot(t,z0,'b');
plot(t,z0-T,'k');
plot(t,z0+T,'g');
plot(t,z0-Tc/2,'y');
plot(t,z0+Tc/2,'y');

subplot(2,2,2),plot(t,E);
hold on;
grid on;

subplot(2,2,3),plot(t,I);
hold on;
grid on;

subplot(2,2,4),plot(t,P);
hold on;
grid on;
clear;
```